Received: 16 December 2022 | Revised: 16 June 2023 | Accepted: 29 June 2023

DOI: 10.1002/ecs2.4645

ECOSPHERE
AN ESA OPEN ACCESS JOURNAL

ARTICLE

Freshwater Ecology

# Identifying drivers of population dynamics for a stream breeding amphibian using time series of egg mass counts

**Jonathan P. Rose**[1] | **Sarah J. Kupferberg**[2] | **Ryan A. Peek**[3,4] | **Don Ashton**[5] | **James B. Bettaso**[6] | **Steve Bobzien**[7] | **Ryan M. Bourque**[8,9] | **Koen G. H. Breedveld**[10] | **Alessandro Catenazzi**[11] | **Joseph E. Drennan**[12] | **Earl Gonsolin**[13] | **Marcia Grefsrud**[14] | **Andrea E. Herman**[15] | **Matthew R. House**[9] | **Matt R. Kluber**[9] | **Amy J. Lind**[16] | **Karla R. Marlow**[12] | **Alan Striegle**[17] | **Michael van Hattem**[8] | **Clara A. Wheeler**[18] | **Jeffery T. Wilcox**[19] | **Kevin D. Wiseman**[20] | **Brian J. Halstead**[21]

[1]U.S. Geological Survey, Western Ecological Research Center, Santa Cruz Field Station, Santa Cruz, California, USA

[2]Independent Scholar and Consulting Ecologist, Berkeley, California, USA

[3]Center for Watershed Sciences, University of California, Davis, California, USA

[4]California Department of Fish and Wildlife, Wildlife Program, Sacramento, California, USA

[5]McBain Associates, Applied River Sciences, Arcata, California, USA

[6]USDA Forest Service, Six Rivers National Forest, Willow Creek, California, USA

[7]East Bay Regional Park District, Stewardship Department, Oakland, California, USA

[8]California Department of Fish and Wildlife, Habitat Conservation Program, Northern Region, Eureka, California, USA

[9]Green Diamond Resource Company, Korbel, California, USA

[10]Spring Rivers Ecological Sciences LLC, Cassel, California, USA

[11]Department of Biological Sciences, Florida International University, Miami, Florida, USA

[12]Garcia and Associates (GANDA), San Francisco, California, USA

[13]Alluvion Biological Consulting LLC, San Jose, California, USA

[14]Bay Delta Region, Habitat Conservation, California Department of Fish and Wildlife, Fairfield, California, USA

[15]Pacific Gas and Electric Company, Oakland, California, USA

[16]USDA Forest Service, Pacific Southwest Region, Nevada City, California, USA

[17]Natural Resources and Lands Management Division, San Francisco Public Utilities Commission, Sunol, California, USA

[18]USDA Forest Service, Pacific Southwest Research Station, Arcata, California, USA

[19]Sonoma Mountain Ranch Preservation Foundation, Petaluma, California, USA

[20]Department of Herpetology, California Academy of Sciences, San Francisco, California, USA

[21]U.S. Geological Survey, Western Ecological Research Center, Dixon Field Station, Dixon, California, USA

**Correspondence**
Jonathan P. Rose
Email: jprose@usgs.gov

## Abstract

The decline in amphibian populations is one of the starkest examples of the biodiversity crisis. For stream breeding amphibians, alterations to natural flow

**Present address**
Clara A. Wheeler, USDA Forest Service, Pacific Northwest Research Station, Portland, Oregon, USA.

**Funding information**
U.S. Fish and Wildlife Service; U.S. Geological Survey

**Handling Editor:** Andrew M. Kramer

regimes by dams, water diversions, and climate change have been implicated in declines and extirpations. Identifying drivers of amphibian declines requires long time series of abundance data because amphibian populations can exhibit high natural variability. Multiple population viability analysis (MPVA) models integrate abundance data and share information from different populations to estimate how environmental factors influence population growth. Flow alteration has been linked to declines and extirpations in the Foothill Yellow-legged Frog (*Rana boylii*), a stream breeding amphibian native to California and Oregon. To date, no study has jointly analyzed abundance data from populations throughout the range of *R. boylii* in an MPVA model. We compiled time series of egg mass counts (an index of adult female abundance) from *R. boylii* populations in 36 focal streams and fit an MPVA model to quantify how streamflow metrics, stream temperature, and surrounding land cover affect population growth. We found population growth was positively related to stream temperature and was higher in the years following a wet year with high total annual streamflow. Density dependence was weakest (i.e., carrying capacity was highest) for streams with high seasonality of streamflow and intermediate rates of change in streamflow during spring. Our results highlight how altered streamflow can further increase the risk of decline for *R. boylii* populations. Managing stream conditions to better match natural flow and thermal regimes would benefit the conservation of *R. boylii* populations.

**KEYWORDS**
amphibian conservation, flow regimes, Foothill Yellow-legged Frog, multiple population viability analysis, population modeling, *Rana boylii*

## INTRODUCTION

The synergistic effects of climate change, introduced species, disease, contaminants, and habitat alteration have driven declines in many species. Amphibians have experienced declines globally (Stuart et al., 2004) and across North America (Grant et al., 2016). Recently, the emphasis of amphibian conservation research has shifted from documenting declines to identifying drivers of population trends (Grant et al., 2020). Identifying factors causing population declines and projecting future population trajectories in the face of stressors necessitate a model of population dynamics. Population dynamics models are often parameterized with data from one or a few populations that have been intensively studied for a long time (Wenger et al., 2017). The transferability of insights from spatially restricted studies to other populations is fraught with complications. The mean growth rate and degree of environmental stochasticity might vary over time and among populations in different climates, disturbance regimes, or habitats (Coulson et al., 2001). Amphibian populations in particular exhibit high natural variation in abundance, necessitating long time series to separate stochastic fluctuations from deterministic trends (Pechmann et al., 1991) and to identify density dependence (Băncilă et al., 2016). Thus, adequately characterizing the drivers of population trends requires data from several populations that encompass the range of conditions experienced by a species.

Multiple population viability analysis (MPVA) is a method for simultaneously modeling multiple populations to infer a species' population dynamics across a wider region (Wenger et al., 2017). In MPVA, data from multiple populations inform estimates of covariate effects on population growth, and estimates of environmental stochasticity can be shared among populations via random effects. This information sharing allows for insights into the dynamics of populations with short time series data, which would not be possible in a single-population approach. Expanding the spatial coverage of population analyses with MPVA can help meet the needs of species status assessments (SSAs) performed by the U.S. Fish and Wildlife Service (Smith et al., 2018) by identifying covariates of population growth parameters. SSAs often employ demographically

structured population models (McGowan et al., 2017), but such demographic data are unavailable for many amphibians. When demographic data are lacking, counts from regular population censuses can be used to estimate population growth (Molano-Flores & Bell, 2012). Count-based models have been applied to wildlife populations for the past four decades; these models can incorporate density dependence (Dennis & Taper, 1994), observation error (Staples et al., 2004), and incomplete sampling (Leasure et al., 2019). Given the greater spatial and temporal coverage of count data, count-based MPVA has the potential to reveal the drivers of population dynamics for many amphibian species.

Alterations to streamflow and impairment by dams threaten freshwater biodiversity globally (Bunn & Arthington, 2002; Poff et al., 2007). For stream-dwelling amphibians in particular, flow conditions determine survival and recruitment success (Lowe et al., 2019; Rose et al., 2021). Alteration to natural flow regimes by dams and water diversions is a major stressor (Dare et al., 2020; Eskew et al., 2012) that can lead to reduced amphibian species richness (Guzy et al., 2018). Dams can change the magnitude of streamflow, the timing of seasonal flows, and water temperatures, with concomitant effects on in-stream and riparian habitats (Poff et al., 1997). Rivers without dams are also expected to experience changes to natural flow regimes (Grantham et al., 2018) as extreme precipitation events and multiyear droughts become more common with ongoing climate change (Huang et al., 2020; Kwon & Lall, 2016; Swain et al., 2018). These alterations can negatively affect amphibians adapted to survive and breed following the natural seasonal streamflow regime (Lowe, 2012).

The Foothill Yellow-legged Frog (*Rana boylii*) is an obligate stream breeding frog native to western North America across a latitudinal cline from Oregon and California, USA, to Baja California, Mexico. *R. boylii* has declined in the past century, particularly in the southern half of its range (Adams et al., 2017; Jennings & Hayes, 1994), leading to the listing of populations in the northern Sierra Nevada (hereinafter the "Northern Sierra" region) and vicinity of the Feather River ("North Feather") as threatened, and populations in the southern Sierra Nevada ("Southern Sierra"), Central Coast, and South Coast as endangered under the California Endangered Species Act (California Fish and Game Commission, 2020). The species is designated as a "sensitive species" by the Oregon Department of Fish and Wildlife (ODFW, 2019), and the U.S. Fish and Wildlife Service proposed listing of four distinct population segments under the U.S. Endangered Species Act (U.S. Fish and Wildlife Service, 2021a). Even within the North Coast region where the species does not appear to be under threat of regional extirpation, occupancy and population density vary greatly among stream reaches both within and between watersheds (Catenazzi & Kupferberg, 2017; Linnell & Davis, 2021; U.S. Fish and Wildlife Service, 2021b).

One of the major drivers of population dynamics for *R. boylii* is the flow regime. In unregulated streams, adult frogs migrate from overwintering sites in tributary streams, seeps, springs, and under terrestrial cover to breeding reaches after the cessation of high winter and spring flows where females deposit egg masses in shallow, low-velocity sites with boulder or cobble substrate. In unregulated streams, eggs and tadpoles develop through late spring and summer as the stream flow slowly recedes (Kupferberg, 1996; van Hattem et al., 2021). In regulated rivers where dams alter flow regimes, aseasonal flow fluctuations can create high-velocity conditions or rapid stage changes that reduce recruitment by scouring or stranding early life stages (Kupferberg et al., 2012; Lind et al., 1996). Dams also produce flow conditions that can allow non-native predators to flourish (Fuller et al., 2011; Light, 2003). Summer water temperatures can be colder in regulated streams because of hypolimnetic releases of water from deep reservoirs, slowing growth and development of tadpoles (Catenazzi & Kupferberg, 2013, 2017; Wheeler et al., 2015). In addition to altered flow regimes, the absence of *R. boylii* from sites within its historical range has been linked to habitat destruction, disease, introduced species, agricultural land use and pesticide spraying upwind from streams, and the use of splash dams to move timber (Adams et al., 2017; Davidson et al., 2002; Linnell & Davis, 2021; Moyle, 1973). Given the observed declines and extirpations, and the variation in population density among extant populations, there is a need for a quantitative assessment of how population growth is related to stream and watershed characteristics.

In this study, we developed an MPVA for *R. boylii* using 36 time series of egg mass counts to estimate how streamflow, stream temperature, and land cover in the surrounding landscape influence population growth, density dependence, and environmental stochasticity in *R. boylii* populations. We focused our models on explanation of observed historical patterns rather than prediction of future population trajectories. Our findings have implications for the management of streams to improve viability and prevent further range contraction of this declining anuran.

# METHODS

## Study region

Recent studies have defined six distinct genetic clades within *R. boylii* corresponding to geographic regions

(McCartney-Melstad et al., 2018; Peek, 2018). We compiled egg mass count data from *R. boylii* populations in five of these regions: (1) the North Coast of California ($n = 20$), (2) Northern Sierra ($n = 5$), (3) North Feather ($n = 2$), (4) Southern Sierra ($n = 2$), and (5) Central Coast ($n = 7$; Table 1; Figure 1). No time series of egg mass counts were available from Oregon or from the South Coast clade, where most populations have been extirpated (Adams et al., 2017; California Department of Fish and Wildlife, 2019). Although the entire range of the species experiences wet winter–dry summer conditions, each region differs in the primary drivers of peak runoff and belowground water storage capacity that determines base streamflow (Hahm et al., 2019; Yarnell et al., 2016). In the South, Central, and North coastal regions, winter and spring rainfall provide most of the water input for streams. In the Northern Sierra, Southern Sierra, and North Feather regions, more precipitation falls as snow at higher elevations, and snowmelt during spring and summer provides the main input for streamflow. In all five regions studied here, natural flow regimes exhibit a recession in flow during spring and summer; transitioning from dynamic winter peaks to a stable summer low baseflow.

## Egg mass surveys

Egg mass surveys are a primary means of monitoring *R. boylii* populations. Females typically lay a single clutch of eggs in a year, and therefore the number of egg masses is a proxy for the number of breeding females in a population (Kupferberg et al., 2012; Zweifel, 1955) and clutch counts correspond with estimates of adult female numbers from capture–mark–recapture efforts for *R. boylii* (Van Wagner, 1996). We compiled time series of egg mass data from surveys of 36 stream reaches lasting from 2 to 30 years (mean = 10.1, SD = 6.9) from 1991 to 2021 (Table 1). Female *R. boylii* begin oviposition as streamflow declines and water temperatures increase in the spring (Kupferberg, 1996; Wheeler et al., 2015); oviposition can last from 2 to 7.5 weeks (Kupferberg, 1996; Wheeler & Welsh, 2008). At a few reaches, egg masses were counted during multiple, up to 7, surveys in a given year, and egg masses were marked to prevent double counting. For most sites, only a single count is available for each year, but the timing of surveys was chosen in an attempt to take place after oviposition had finished. Because complete hatching of a clutch and the resulting disintegration of the egg jelly takes a few to several weeks after oviposition (depending on temperature; Hayes et al., 2016; Kupferberg et al., 2011; Zweifel, 1955), timing surveys this way observes the output of early breeders and avoids missing egg masses laid later in the spring. For consistency, for all sites, we used the total count of unique egg masses observed that year as the input data for the model. Time series of egg mass counts were not continuous for some streams, but state-space models that underlie MPVA (see below) allow for the use of incomplete time series by inferring the abundance of egg masses during years without surveys. Egg mass surveys came from a variety of sources, including long-term studies of the ecology of *R. boylii* (e.g., Kupferberg et al., 2012; Wheeler & Welsh, 2008), monitoring programs for populations affected by dams (e.g., Pacific Gas and Electric Company, 2020; Snover & Adams, 2016), and focused studies on the effects of environmental conditions on breeding (e.g., Gonsolin, 2010; Lind et al., 1996; van Hattem et al., 2021; Wheeler et al., 2015). We treated reaches of the same stream as a single population if they were directly connected without any barrier (e.g., a dam, lake, or reservoir) between the reaches and were surveyed using the same methods by the same research group. If two reaches were consecutive along the same stream but separated by a dam that created different flow conditions in the upper and lower reach, we treated those two reaches as separate populations (e.g., Alameda Creek above and below the regulated release from Calaveras Dam near Sunol, CA, USA). Likewise, surveyed reaches from a tributary were treated as independent populations from surveyed reaches in the mainstem river (e.g., the mainstem, South Fork, and North Fork of the Trinity River were treated as three separate populations).

## Count-based MPVA

We fit a state-space MPVA model to the egg mass count time series data in a Bayesian framework that shares information among populations to better estimate true population growth rates and observation error in counts. State-space models are widely used to analyze population time series data because they enable the simultaneous fitting of process and observation models (de Valpine & Hastings, 2002; Knape et al., 2011). Our MPVA (Figure 2) was modified from the model developed by Leasure et al. (2019) for Lahontan Cutthroat Trout (*Oncorhynchus clarkii henshawi*). The MPVA comprises three submodels: a process model, a sampling model, and an observation model. The process model describes the change in the true abundance of adult female frogs over time and is used to estimate the population growth rate, the strength of density dependence, and the effect of environmental covariates on each. At some sites, the length of stream reach surveyed varied between years. We used a sampling model to relate the surveyed reach to the maximum extent of stream surveyed in a single year. Finally, because counts of egg masses are an imperfect measure

**TABLE 1** Characteristics of streams with time series of *Rana boylii* egg mass counts.

| Site no. | Stream reach | Years surveyed | Reg | Reach extent (km) | Mean egg mass density | Total annual streamflow ($m^3$) | Total upstream drainage area ($km^2$) |
|---|---|---|---|---|---|---|---|
| Central Coast | | | | | | | |
| 1 | Alameda Creek—Ohlone* | 1997–2021 | N | 1.23 | 17.9 | 1.79E+07 | 87.4 |
| 2 | Alameda Creek—Sunol | 2003–2020 | Y | 3.69 | 5.2 | 2.22E+07 | 361.3 |
| 3 | Alameda Creek—3 | 2016–2021 | Y | 1.14 | 21.2 | 2.22E+07 | 371.8 |
| 4 | Alameda Creek—4 | 2008, 2014, 2016–2021 | Y | 1.21 | 21.8 | 1.16E+07 | 92.9 |
| 5 | Alameda Creek—5* | 2016–2021 | N | 0.81 | 32.3 | 1.79E+07 | 83.9 |
| 6 | Arroyo Hondo* | 2007, 2011, 2014–2021 | N | 4.67 | 21.3 | 4.16E+07 | 203.2 |
| 7 | Coyote Creek* | 2004–2005, 2019, 2021 | N | 4.84 | 21.3 | 3.19E+07 | 197.0 |
| North Coast | | | | | | | |
| 8 | Big Carson Creek* | 2004–2021 | N | 1.27 | 13.8 | 2.22E+06 | 5.1 |
| 9 | Browns Creek* | 2013–2017 | N | 0.4 | 8.5 | 7.75E+07 | 190.7 |
| 10 | Canyon Creek* | 2013–2016 | N | 0.4 | 65 | 1.19E+08 | 166.0 |
| 11 | Copeland Creek* | 2016, 2018–2021 | N | 0.93 | 8.6 | 3.35E+06 | 4.0 |
| 12 | Hurdygurdy Creek | 1991–1992, 1998–2000, 2002–2008 | N | 4.7 | 28.3 | 3.11E+09 | 77.4 |
| 13 | Indian Creek* | 2013–2017 | N | 0.4 | 32.5 | 2.77E+07 | 87.3 |
| 14 | Little Carson Creek* | 2004–2021 | N | 1.75 | 6.5 | 1.73E+06 | 3.7 |
| 15 | Mad River | 2008–2020 | N | 3.03 | 241 | 1.12E+09 | 1258.7 |
| 16 | Mainstem Trinity River | 1991–1994, 2004–2009, 2013–2017 | Y | 36.2 | 1.02 | 7.10E+08 | 1862.2 |
| 17 | NF Trinity River* | 2004–2006, 2008–2009, 2013–2017 | N | 1.61 | 77.4 | 2.80E+08 | 394.5 |
| 18 | Oregon Gulch* | 2013–2017 | N | 0.4 | 19 | 8.25E+06 | 19.3 |
| 19 | Pit River | 2003–2005, 2007–2020 | Y | 11.5 | 5 | 5.72E+08 | 10827.2 |
| 20 | Reading Creek* | 2013–2017 | N | 0.4 | 5.5 | 4.15E+07 | 80.6 |
| 21 | Redwood Creek | 2011–2012 | N | 14.1 | 19.2 | 7.89E+08 | 724.3 |
| 22 | San Anselmo Creek | 2018–2021 | N | 1.5 | 5.8 | 5.13E+06 | 9.5 |
| 23 | SF Eel River—Angelo | 1992–2021 | N | 5.2 | 108.2 | 2.05E+07 | 149.6 |
| 24 | SF Eel River—Benbow | 2012–2013, 2015–2019, 2021 | N | 3.6 | 148.1 | 1.38E+09 | 1132.2 |
| 25 | SF Trinity River | 1992–1994, 2004–2009 | N | 15.6 | 87.2 | 1.06E+09 | 1982.7 |
| 26 | Tenmile Creek | 1993–2003, 2008–2010 | N | 1 | 27.4 | 2.05E+07 | 169.4 |
| 27 | Weaver Creek* | 2013–2017 | N | 0.4 | 18.5 | 6.35E+07 | 128.7 |
| North Feather | | | | | | | |
| 28 | NF Feather River—Cresta | 2002–2021 | Y | 7.17 | 1.7 | 7.76E+08 | 4961.7 |
| 29 | NF Feather River—Poe | 2001–2021 | Y | 12.38 | 7.2 | 1.71E+09 | 5083.7 |
| Northern Sierra | | | | | | | |
| 30 | American Canyon Creek | 2010–2013 | N | 0.31 | 28.2 | 2.27E+06 | 9.2 |

(Continues)

**TABLE 1** (Continued)

| Site no. | Stream reach | Years surveyed | Reg | Reach extent (km) | Mean egg mass density | Total annual streamflow ($m^3$) | Total upstream drainage area ($km^2$) |
|---|---|---|---|---|---|---|---|
| 31 | NF American River | 2009, 2011–2017, 2019–2021 | N | 0.9 | 45.7 | 7.05E+08 | 888.1 |
| 32 | North Yuba River | 2012–2015 | N | 0.8 | 22.2 | 6.54E+08 | 652.1 |
| 33 | Rubicon River | 2009, 2011–2015 | Y | 1 | 25 | 4.82E+07 | 293.9 |
| 34 | South Yuba River | 2013–2014 | Y | 0.4 | 12.5 | 1.10E+08 | 319.8 |
| Southern Sierra | | | | | | | |
| 35 | NF Mokelumne River | 2001–2003, 2010–2014, 2017–2018 | Y | 2.7 | 3 | 2.05E+08 | 707.2 |
| 36 | MF Stanislaus River | 2010–2014 | Y | 4.32 | 2.9 | 3.01E+08 | 854.2 |

*Note*: Extent is the length of the longest reach surveyed during the time series, but the extent of surveys varied among years at some sites. Regulated status (Reg) is determined by whether there is a dam upstream of the study reach (Y) or not (N), resulting in an upstream degree of regulation >10%. An asterisk denotes streams with downstream dams. Mean egg mass density is the average number of egg masses per stream kilometers over the sample period for each stream. Site number corresponds to values depicted in Figure 1. Total annual streamflow is the cumulative stream discharge for an average year in cubic meters (see data sources in Appendix S1: Table S1). Total upstream drainage area (in square kilometers) is the total upstream cumulative drainage area at the downstream end of the reach, from the NHDPlus version 2 dataset (McKay et al., 2012).

of abundance, we used an observation model to relate the observed egg mass counts to the true, unobserved adult female abundance. Failing to account for observation error can lead to overestimating the strength of density dependence in population time series (Freckleton et al., 2006; Knape & de Valpine, 2012), but the type of observation error assumed might have little influence on parameter estimates (Schmidt et al., 2021). We describe the process model in detail below, and descriptions of the sampling and observation models can be found in Appendix S1.

## Process model

In the process model, adult female abundance changes according to a Ricker model with density dependence (Ricker, 1954). The classical form of the Ricker model, $N_t = N_{t-1}e^{r\left(1-\frac{N_{t-1}}{K}\right)}$, defines population growth from year $t-1$ to year $t$ based on the intrinsic population growth rate, $r$, and the carrying capacity of the environment, $K$. We used an alternative form of the Ricker model (Equation 1) where density dependence is defined as $\phi = -r/K$ to enable estimation of covariate effects on $r$ and $\phi$ (Hobbs & Hooten, 2015; Leasure et al., 2019).

$$\log\left(\overline{N}_{p,t}\right) = \log\left(N_{p,t-1}\right) + r_{p,t} + \phi_{p,t} \times \frac{N_{pt-1}}{E_p}. \quad (1)$$

$N_{p,t}$ is the true abundance of population $p$ in year $t$, $E_p$ is the total extent of stream habitat (breeding and nonbreeding habitat) in population $p$, and $r_{p,t}$ and $\phi_{p,t}$ are the intrinsic population growth rate and strength of density dependence for population $p$ in year $t$, respectively. More negative values of $\phi$ represent stronger density dependence and a lower carrying capacity, and more positive values of $\phi$ represent weaker density dependence and a higher carrying capacity. This is a first-order autoregressive model, and $N_{p,t}$ depends only on the abundance at the previous time step, $N_{p,t-1}$. An implicit assumption of our model is that all female *R. boylii* alive in year $t$ lay egg masses, and therefore changes in $N$ between years reflect real changes in abundance, not changes in the number of females that are breeding. The expected realized population growth rate $\overline{R}_{p,t}$ is then a function of $r_{p,t}$, $\phi_{p,t}$ and the density of population $p$ in year $t-1$ (Equation 2).

$$\overline{R}_{p,t} = r_{p,t} + \phi_{p,t} \times \frac{N_{p,t-1}}{E_p}. \quad (2)$$

By scaling the density-dependence term by population density ($N/E$), instead of abundance, the $\phi$ term is comparable among populations with different spatial extents. This form of the Ricker model avoids identifiability issues that result from modeling spatial and temporal variation in $r$ and $K$ and allows for the inclusion of covariates on $r$ and $\phi$ (Wenger et al., 2017; Equation 3). In Equation (3), $\boldsymbol{X}_{p,t}$ is a matrix of covariates on population growth, $\beta_r$ is a vector of slopes, $\alpha_r$ is the average population growth, and $\varepsilon_{r,c}$ are region random effects on $r$. To account for potential differences among

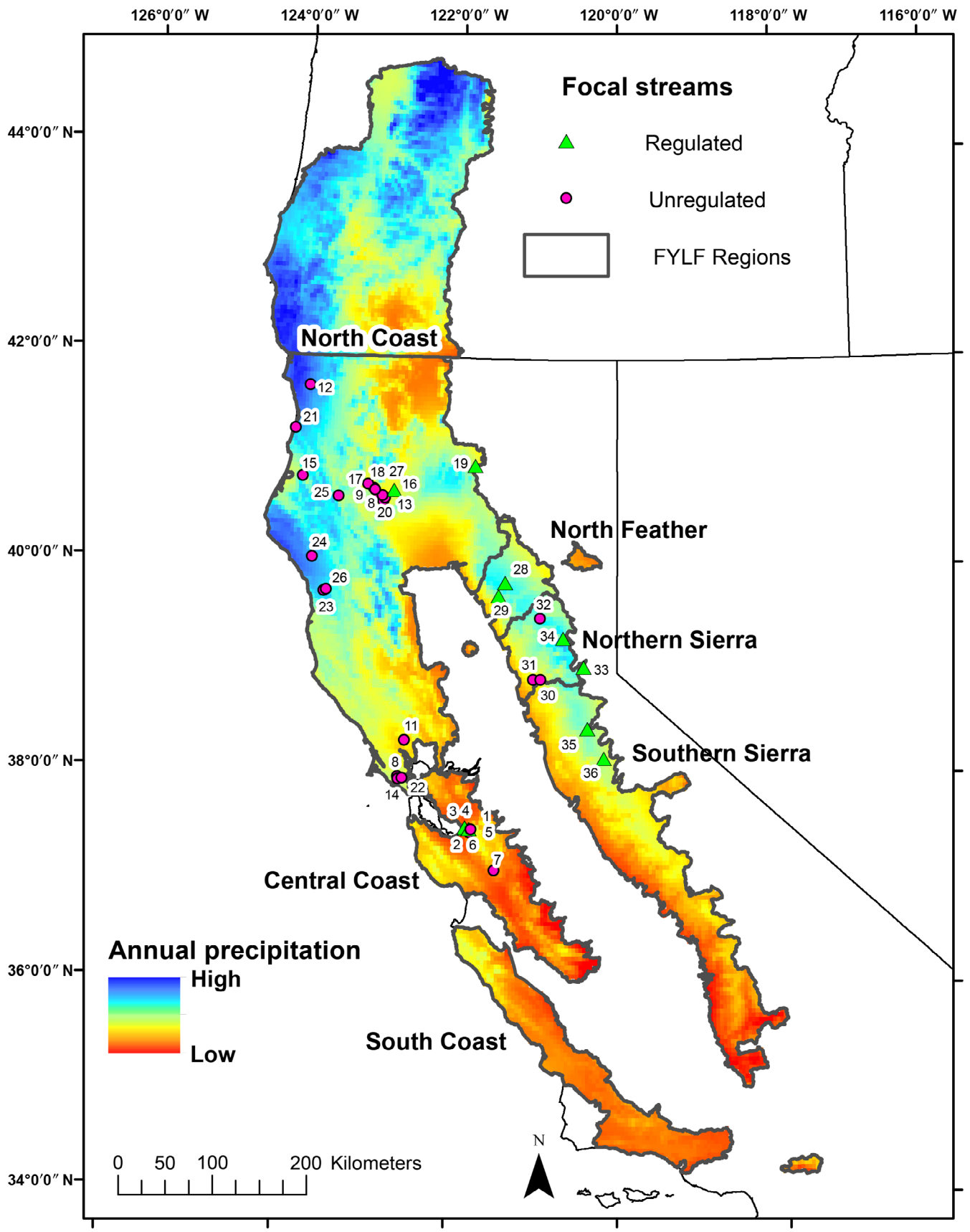


**FIGURE 1** Location of focal streams with time series of egg mass counts for *Rana boylii* (foothill yellow-legged frog, FYLF) collected from 1991 to 2021. Data from these 36 streams were used to fit the multiple population viability analysis model. Polygons represent the range of *R. boylii* clades and management regions defined by the U.S. Fish and Wildlife Service. Labeled numbers correspond to site numbers in Table 1.

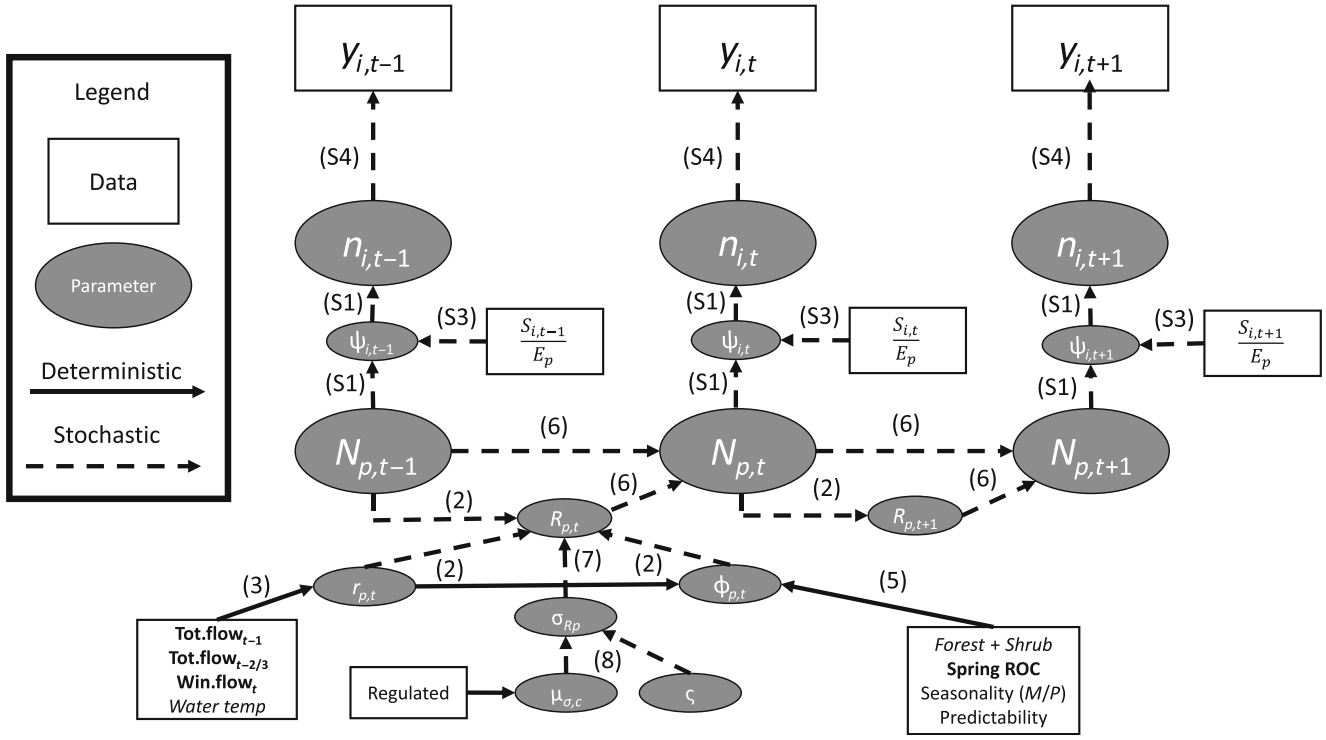


**FIGURE 2** A conceptual model (directed acyclic graph) of the hierarchical multiple population viability analysis for *Rana boylii*. Empirical data are in plain text, modeled data are in italics, and bold font indicates data are a mix of empirical and modeled. Numbers in parentheses correspond to numbered equations presented in the main text. Inputs to the realized growth rate are only shown for the first time period ($R_{p,t}$) but apply equally to the second period ($R_{p,t+1}$). Parameter definitions are as follows: $y_{i,t}$ is the observed egg mass counts at reach $i$ in year $t$; $n_{i,t}$ is the true abundance of female frogs at reach $i$ in year $t$; $\psi_{i,t}$ is the probability an individual in population $p$ occurred in the surveyed reach $i$ in year $t$; $S_{i,t}$ is the length of reach $i$ surveyed in year $t$; $E_p$ is the total extent of habitat at population $p$; $N_{p,t}$ is the true abundance of female frogs in population $p$ in year $t$; $R_{p,t}$ is the realized growth rate for population $p$ in year $t$; $r_{p,t}$ is the intrinsic growth rate for population $p$ in year $t$; $\phi_{p,t}$ is the strength of density dependence for population $p$ in year $t$; $\sigma_{R,p}$ is the standard deviation of environmental stochasticity in $R$ for population $p$; $\mu_{\sigma,c}$ is the mean environmental stochasticity for a region and regulation class $c$; $\varsigma$ is the standard deviation of the reach random effect on $\sigma_R$. Environmental covariates are defined as follows: Tot.flow$_{t-1}$ is the standardized total annual streamflow deviation in year $t-1$, Tot.flow$_{t-2/3}$ is the standardized total annual streamflow deviation in year $t-2$ or $t-3$ depending on the region; Win.flow$_t$ is the standardized peak winter streamflow in year $t$; Water temp is the mean model-predicted August stream temperature; Regulated is a binary indicator if a stream reach is regulated by an upstream dam or not; Forest + Shrub is the total proportion of the surrounding 8-digit Hydrologic Unit Code sub-basin that is covered with forest or shrubland habitats; Spring ROC is the percentage of rate of change in the spring recession flow; Seasonality ($M/P$) is the ratio of Colwell's $M$ (contingency) to Colwell's $P$ (predictability) metrics for time series data; Predictability is the predictability of streamflow at a 12-month time interval based on the proportion of wavelet power that is significant at the $\alpha = 0.01$ level.

regions (i.e., clades) in the intrinsic population growth rate, we included region random effects on $r$ ($\varepsilon_{r,c}$), which are drawn from a normal distribution with a SD of $\kappa_r$ (Equation 4). In Equation 5, $\gamma_\phi$ is the average density dependence, $\theta_\phi$ is a vector of slopes, and $\mathbf{Z}_{p,t}$ is a matrix of covariates on the strength of density dependence. We did not include a region random effect on $\phi$ because we expected the strength of density dependence to be explained by environmental drivers of the carrying capacity of a particular stream, rather than differences among clades per se. For example, the abundance of stream salamanders in North Carolina was related to the degree of disturbance in the watershed (Willson & Dorcas, 2003), and stream-dwelling amphibian density in northern California was influenced by disturbance from sediment deposition (Welsh & Ollivier, 1998).

$$r_{p,t} = \alpha_r + \beta_r \boldsymbol{X}_{p,t} + \varepsilon_{r,c}. \quad (3)$$

$$\varepsilon_{r,c} \sim N(0, \kappa_r). \quad (4)$$

$$\phi_{p,t} = \gamma_\phi + \theta_\phi \boldsymbol{Z}_{p,t}. \quad (5)$$

The abundance and realized population growth rates have a stochastic component in addition to the deterministic component in Equations (1) and (2), because demographic stochasticity can be an important process for small populations (Melbourne & Hastings, 2008). We

modeled demographic stochasticity using a Poisson process, where the true abundance for population $p$ in year $t$ is drawn from a Poisson distribution centered on the expected abundance (Equation 6).

$$N_{p,t} \sim \text{Poisson}\left(N_{p,t-1}e^{R_{p,t}}\right). \quad (6)$$

Environmental stochasticity represents spatiotemporal variation in demographic rates that is driven by unmeasured, exogenous environmental factors (Melbourne & Hastings, 2008). We modeled environmental stochasticity using a normal distribution for realized population growth rates, centered on the expected realized growth rate (Equation 7). The SD of environmental stochasticity, $\sigma_{R_p}$, was used to account for variance that is not explained by environmental covariates on $r$ and $\phi$.

$$R_{p,t} \sim \text{Normal}\left(\overline{R}_{p,t}, \sigma_{R_p}\right). \quad (7)$$

The SD of environmental stochasticity for each population, $\sigma_{R_p}$, was a random effect drawn from a shared half-Cauchy distribution for all study populations (Equation 8). Treating environmental stochasticity as a random effect enables sharing information about variation in growth rates among populations and can improve precision for populations lacking long time series. The mean environmental stochasticity, $\mu_{\sigma,c}$, was allowed to vary among regions using a random effect centered on an overall mean for that regulation class (i.e., separate means for regulated and unregulated streams), $\omega_\sigma$ (Equation 9).

$$\sigma_{R_p} \sim \text{halfCauchy}\left(\mu_{\sigma,c}, \varsigma\right). \quad (8)$$

$$\mu_{\sigma,c} \sim \text{Normal}\left(\omega_\sigma, \xi\right). \quad (9)$$

Streams were classified as regulated if the upstream degree of regulation (Cooper et al., 2017) was >10% and unregulated otherwise. We chose the 10% threshold based on a comparison of upstream degree of regulation values to the presence of upstream dams and our knowledge of the focal streams' flow regimes.

## Environmental covariates

We selected a set of environmental covariates to avoid overfitting the model to our sample of 36 focal streams and identify general relationships with environmental factors we expected to have similar effects on *R. boylii* populations across regions. We included measures of total annual streamflow (discharge; for the water year from October 1 to September 30), peak winter streamflow (December 1–March 30), and average summer stream temperatures for the stream segment (National Hydrography Dataset, U.S. Geological Survey, 2019) as environmental covariates on the intrinsic population growth rate, $r$. Details on the source of streamflow data are available in Appendix S1. We included the total annual streamflow from each stream as a covariate on $r$ using two lag times chosen to represent the effects of streamflow on survival of post-metamorphic frogs and recruitment from eggs and tadpoles to reproductively mature frogs. We used a 1-year lag to represent the potential for high flow or low flow years to influence the survival of adult and subadult frogs from year $t-1$ to year $t$. To represent the potential influence of high flow versus low flow years on recruitment, we used a longer lag of either 2 years (expected age at maturity for Central Coast streams; Kupferberg, Lind, et al., 2009) or 3 years (expected age at maturity for North Coast, Northern Sierra, Southern Sierra, and North Feather; Kupferberg, Lind, et al., 2009). For example, if streamflow during spring and summer affects the survival of egg masses and tadpoles in year $t$, and it takes 3 years for individuals to reach sexual maturity, then $r$ in year $t+3$ will be related to streamflow 3 years earlier via recruitment. As an additional streamflow characteristic that could affect overwinter survival of adult and subadult frogs, we calculated the peak winter streamflow for each stream each year. For December through March of each water year, we calculated the maximum daily flow for gaged streams or the maximum of the predicted flow for unregulated streams without gages from the California Unimpaired Flows Database (Zimmerman et al., 2022). Peak winter streamflow in year $t$ was included as a covariate on $r$ for year $t$. Both total annual streamflow and peak winter streamflow were standardized on a per-stream basis (by subtracting the mean for that stream and dividing by the SD for that stream) such that each year had a value indicating the deviation from the average for that stream. We also used the mean predicted August stream temperatures from 1993 to 2015 from the NorWeST dataset (Isaak et al., 2017) as a covariate on $r$ (Appendix S1). Tadpole survival and growth rates in *R. boylii* are positively related to water temperature, and cold water released from dams is known to reduce tadpole growth and survival to metamorphosis (Catenazzi & Kupferberg, 2013, 2017).

We used land cover data and projections from the Land Use and Carbon Scenario Simulator (LUCAS) model (Sleeter et al., 2017, 2019) to quantify the mean forest and shrub cover from 2001 to 2019 within the HUC8 sub-basin (eight-digit Hydrologic Unit Code from the USGS watershed boundary dataset; Jones et al., 2022) containing the focal stream. A sub-basin corresponds to a medium-sized river basin. We used forest and shrub cover as a covariate on $\phi$ because these represent the major natural land cover

types surrounding streams occupied by *R. boylii*. We expected *R. boylii* populations with more forest and shrub cover in the surrounding watershed to be less disturbed and to have higher egg mass densities.

Finally, we included three streamflow metrics as covariates on ϕ. The rate of change for the spring recession flow (Yarnell et al., 2020) is expected to be important for successful recruitment in *R. boylii*, with higher rates of change more likely to cause egg masses and tadpoles to be stranded or scoured (Yarnell et al., 2016). We modeled a quadratic effect of the rate of change of spring recession flow on density dependence in *R. boylii* to allow for a functional relationship where egg mass density is greatest for an intermediate value of spring rate of change. Streamflow regulation by dams in California decreases both the seasonality (how flow varies among seasons within a year) and predictability (how similar are flows at the same time each year) of streamflow, weakens the link between streamflow and natural environmental cues, and results in less genetic connectivity among populations of *R. boylii* (Peek et al., 2021). We quantified the seasonality of streamflow for each focal stream reach using the ratio of Colwell's indices *M* (contingency) to *P* (within-season predictability), where higher values of *M*/*P* indicate greater seasonal differences in streamflow (Colwell, 1974; Peek et al., 2021; Tonkin et al., 2017). We calculated *M* and *P* using the "hydrostats" R package (Bond, 2019). As a metric of predictability of streamflow year over year, we used Wavelet analysis (Torrence & Compo, 1998) to calculate the standardized Morlet power for the streamflow time series at the 12-month time interval and then summarized the proportion of 12-month time steps that had significant power at the $\alpha = 0.01$ level (Tonkin et al., 2017). We calculated Wavelet power using the "WaveletComp" R package (Roesch & Schmidbauer, 2018). Calculating Colwell's *M* and *P* metrics and Wavelet analysis require daily time series data; therefore, we used surrogate stream gage data from nearby streams for unregulated stream reaches lacking gages (Appendix S1: Table S1).

We evaluated the influence of environmental covariates by calculating the proportion of the posterior distribution which was on the same side of zero as the median of the posterior distribution for each coefficient. The greater the proportion of the posterior distribution that was negative (positive) for a coefficient, the greater support for that covariate having a negative (positive) relationship with the response variable (*r* or ϕ).

## Model evaluation

We first evaluated the MPVA's ability to forecast into the immediate future by withholding the last year of data for each population, refitting the model, and comparing predicted counts for the last year to the observed count. As a more stringent test, we also fit the model to the full time series for all sites but one, and for the last site, we withheld the second half of the time series of egg mass counts. We then compared predicted with observed counts for the second half of the time series for that site. This process was repeated for each stream with ≥10 years of egg mass counts ($n = 16$), in a k-fold cross-validation process. For each goodness-of-fit test, we visually assessed the model fit by comparing observed egg mass counts to predicted egg mass counts from the model.

## MPVA model fitting

We fit MPVA models using Markov chain Monte Carlo (MCMC) methods implemented in Just Another Gibbs Sampler (JAGS) software version 4.3.0 (Plummer, 2003) accessed through R version 4.1.3 (R Core Team, 2022) using the "runjags" R package version 2.2.0-3 (Denwood, 2016). The MPVA JAGS code was modified from Leasure et al. (2019); definitions of model parameters and translations between the above equations and JAGS code are provided in Appendix S1: Table S2. We ran the MPVA on four chains for 250,000 iterations each after discarding a burn-in of 20,000 iterations. We thinned the resulting chains by a factor of 10, resulting in a total of 100,000 MCMC samples for inference. We evaluated the mixing of chains by inspecting trace plots and tested for failure of convergence using the potential scale reduction factor, $\widehat{R}$ (Brooks & Gelman, 1998). All model parameters appeared to converge, had effective sample sizes >800, and had $\widehat{R}$ values ≤1.02. Data are available from ScienceBase (Rose et al., 2023, https://doi.org/10.5066/P98K2WJI) and codes to reproduce analyses are available from GitLab (Rose & Halstead, 2023, https://doi.org/10.5066/P9QWX2GR).

# RESULTS

*R. boylii* populations inhabiting unregulated streams exhibited higher egg mass densities on average compared with regulated streams (Figure 3). In the 25 unregulated stream reaches, the average egg mass density over all sites and years was 53.8 egg masses/km (SD = 74.9), compared with just 7.1 egg masses/km (SD = 8.8) in 11 regulated stream reaches (Table 1). In the North Feather and Southern Sierra regions, time series of egg mass counts were only available from regulated streams. In the other three regions, data were available

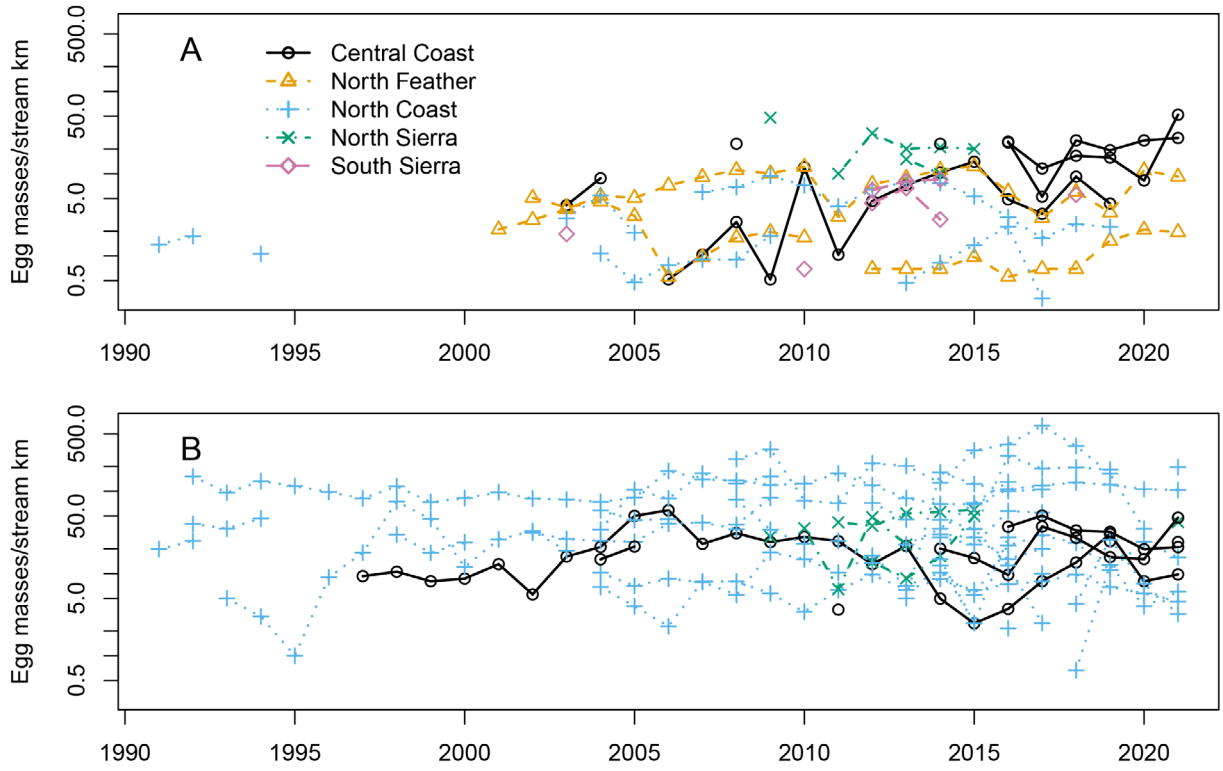


**FIGURE 3** Time series data on the density of egg masses (count of egg masses/stream kilometers surveyed) from *Rana boylii* from 36 focal streams surveyed from 1991 to 2021. (A) Data from regulated streams; (B) data from unregulated streams. Note the *y*-axis is on the log scale.

from both regulated and unregulated streams, although the majority of stream reaches with egg mass data in the North Coast region were unregulated (18 of 20).

Environmental conditions varied by regulation status and by region. Regulated stream reaches generally had distinctive hydrographs compared with unregulated stream reaches, with sharper increases in flow and higher, more stable minimum baseflows (Figure 4). The lowest August stream temperatures were in regulated reaches, and the highest temperatures were in unregulated reaches (Figure 5). On average, regulated stream reaches had lower seasonality and inter-annual predictability of streamflow than unregulated reaches (Figure 6). The average daily rate of change during the spring recession flow did not differ between regulated and unregulated stream reaches, but regulated reaches exhibited greater variability in this streamflow metric, with the highest and lowest rates of change observed in regulated streams (Figure 6). August stream temperatures were highest for reaches in the Central Coast region and lowest in the Northern Sierra region. Stream reaches in the North Coast region exhibited the highest seasonality and inter-annual predictability of streamflow (Appendix S1: Table S3).

## Model validation

The MPVA model performed reasonably well at forecasting one year ahead for a population, given a time series of egg mass counts on which to estimate population-specific parameters (Appendix S1: Figure S1). The 95% credible interval of the predicted egg mass count in the final year of the time series included the observed egg mass count for 30 of 36 populations. The MPVA performed worse when predicting further into the future. When the model was fit to half of the time series for a site, posterior distributions of predicted counts showed good coverage of low observed counts but underestimated the observed count data when real egg mass counts were high (Appendix S1: Figure S2).

## Environmental covariates and population growth

Of the four environmental covariates on $r$, two had strong support for their importance in explaining patterns in the egg mass count data (Figure 5; Table 2). The 1-year lagged effect of standardized total annual flow on $r$ was positive ($\Pr[\beta > 0] = 0.99$). In other words, if 2011

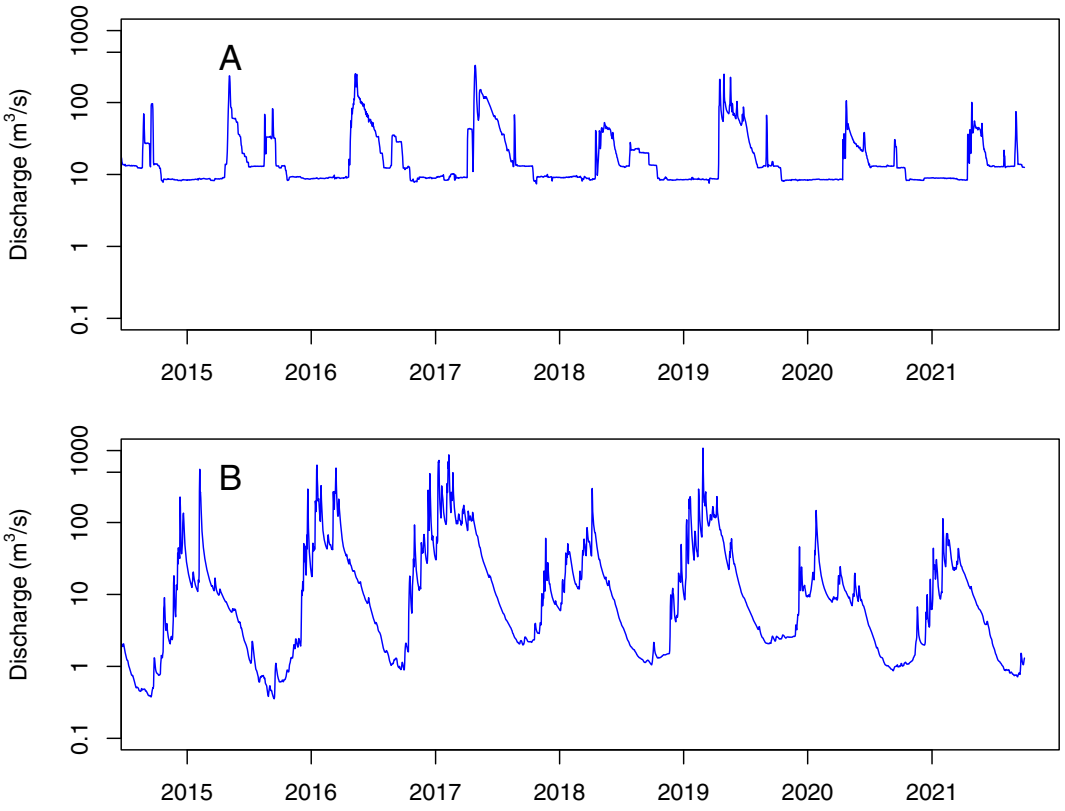


**FIGURE 4** Hydrographs presenting mean daily stream discharge (in cubic meters per second) for the 2015–2021 water years for (A) the regulated Mainstem Trinity River (below Lewiston Dam, NWIS Gage ID 11525500) and (B) the unregulated South Fork Trinity River (below Hyampom, NWIS Gage ID 11528700). The hydrograph for the Mainstem Trinity River exhibits low seasonality ($M/P = 0.60$), whereas the hydrograph for the South Fork Trinity River is highly seasonal ($M/P = 0.91$).

was a wet year with higher total streamflow than average, population growth from 2011 to 2012 was expected to be higher, whereas if 2012 had lower streamflow than average (e.g., in a drought year), population growth from 2012 to 2013 was expected to be lower. Mean August stream temperature was also positively related to $r$ ($\Pr[\beta > 0] = 0.99$), indicating streams with warmer model-predicted temperatures had higher population growth (Figure 5). Support for a positive effect of a 2- or 3-year lagged effect of standardized total annual flow on $r$ ($\Pr[\beta > 0] = 0.83$) and a negative effect of peak winter streamflow on $r$ ($\Pr[\beta < 0] = 0.80$) was weaker.

Seasonality of streamflow had the strongest support for a positive relationship with $\phi$ ($\Pr[\theta > 0] = 0.99$), followed by a quadratic relationship between $\phi$ and spring recession flow rate of change ($\Pr[\theta_{roc} > 0] = 0.92$, $\Pr[\theta_{roc2} < 0] = 0.79$; Table 2). Streams that exhibited greater seasonality in flow had weaker density dependence (i.e., higher carrying capacity) (Figure 6). Streams with intermediate rates of change in flow during the spring recession period had weaker density dependence than streams with high or low rates of change in spring recession flow (Figure 6). Support for positive relationships between $\phi$ and the forest or shrub land cover in the surrounding HUC8 watershed ($\Pr[\theta > 0] = 0.81$) and the inter-annual predictability of streamflow ($\Pr[\theta > 0] = 0.79$) was weaker. The relationship between $\phi$ and predictability was highly uncertain for streams in which predictability was low (predictability <0.8, Figure 6). The amount of residual environmental stochasticity in realized population growth rates varied among streams (Appendix S1: Table S4), with slightly higher average environmental stochasticity for regulated streams compared with unregulated streams (Table 2; $\Pr[\omega_{\sigma,reg} > \omega_{\sigma,unreg}] = 0.80$).

## DISCUSSION

Our analysis of 36 stream reaches with repeated census data for *R. boylii* revealed how population dynamics were related to stream temperature and streamflow. Colder stream temperatures were associated with lower intrinsic growth rates, which is biologically plausible given the faster growth, development, and lower risk of predation for larval *R. boylii* in warmer temperatures (Catenazzi & Kupferberg, 2017, 2018). Regulated stream reaches had

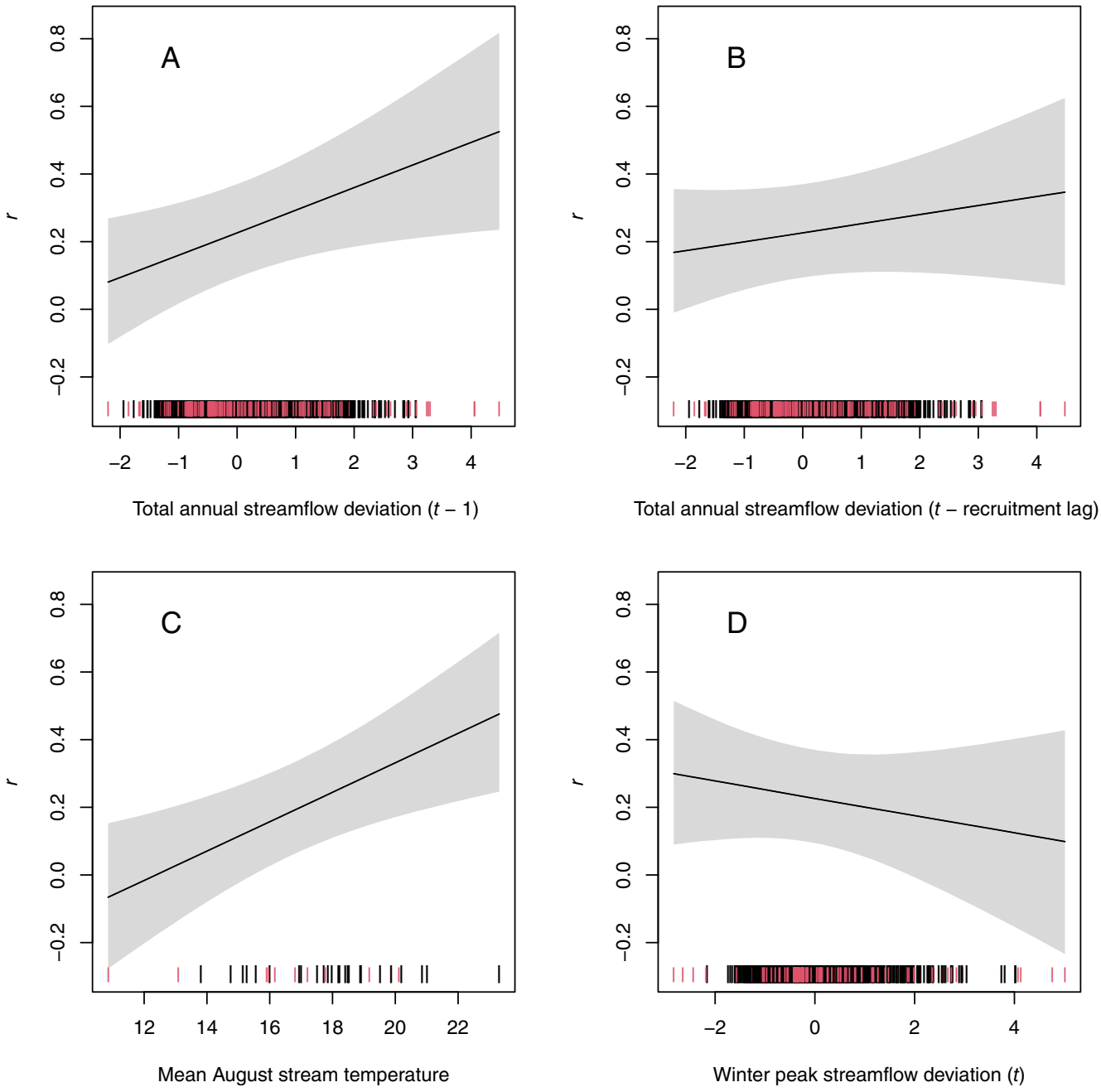


**FIGURE 5** The estimated effect of (A) the standardized total annual streamflow in year $t-1$, (B) the standardized total annual streamflow in year $t-$ recruitment lag (either 2 or 3 years depending on the region), (C) mean August stream temperature, and (D) standardized winter peak streamflow in year $t$ on the intrinsic population growth rate ($r$) from the multiple population viability analysis. Higher values of $r$ represent higher intrinsic population growth rates before accounting for the effects of density dependence. Solid lines represent median predicted relationships, and gray shaded areas represent the 95% credible intervals. Vertical hashes on the $x$-axis represent observed values of environmental covariates from the 36 focal streams (annual values for panels A, B, and D; single values for panel C), red hashes are regulated streams, and black hashes are unregulated streams.

much lower density of egg masses on average. Density dependence was weaker (i.e., higher carrying capacity) in streams with greater seasonality of flow and intermediate rates of change in the spring recession flow. The negative impact of stream regulation on *R. boylii* populations is supported by field studies documenting lower egg mass density, lower survival rates of egg masses, and reduced growth of larval *R. boylii* in regulated rivers (Kupferberg et al., 2012; Lind et al., 1996; Wheeler et al., 2015). Aseasonal pulse flows can lead to high mortality for eggs and tadpoles and are one of the primary ways that flow alteration negatively affects populations of *R. boylii*

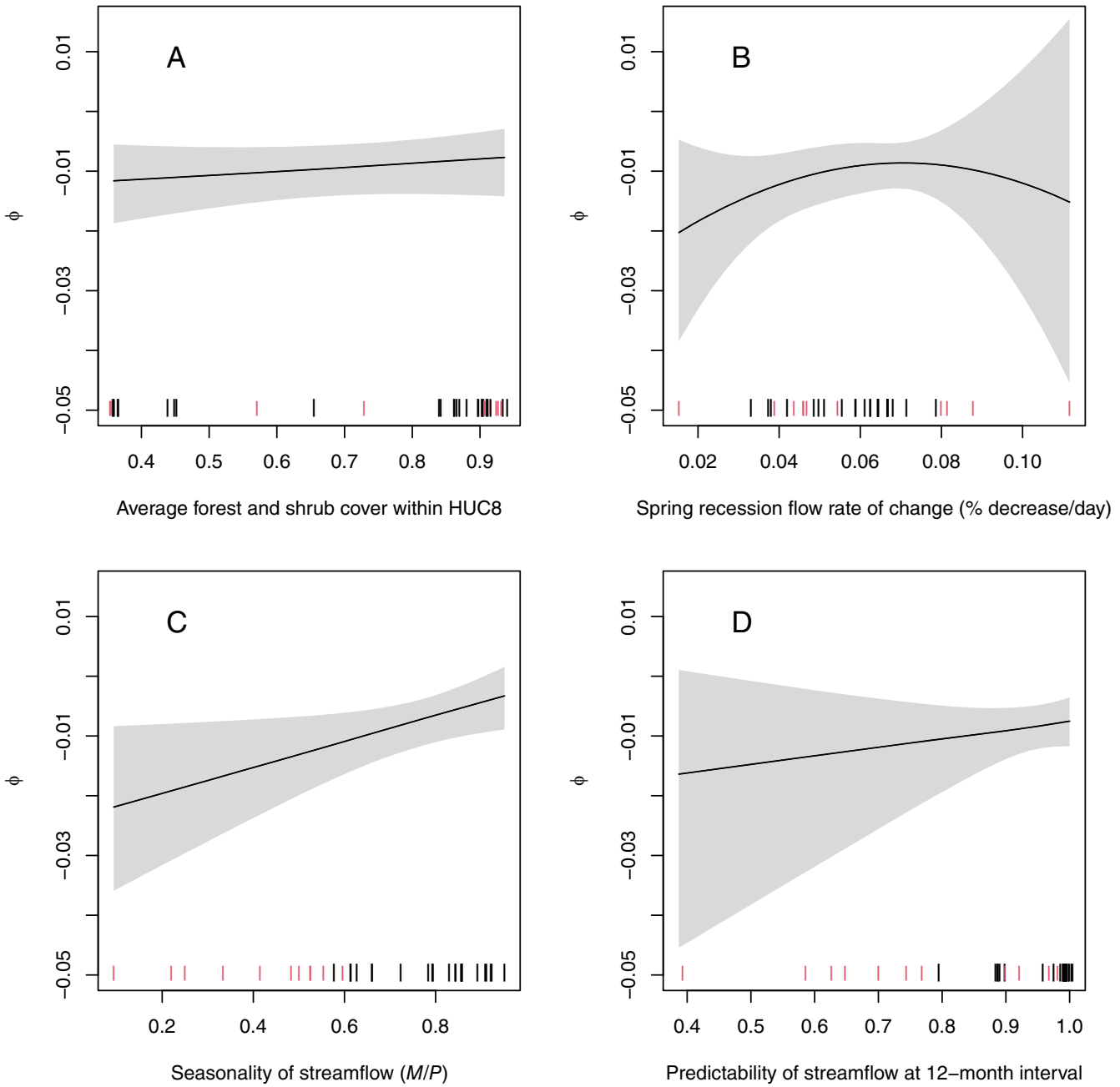


**FIGURE 6** The estimated effect of (A) forest or shrub land cover in the surrounding sub-basin (eight-digit Hydrologic Unit Code, HUC8), (B) daily rate of change in spring recession flow, (C) seasonality of streamflow ($M/P$ or ratio of contingency to within-season predictability), and (D) predictability of streamflow on the strength of density dependence ($\phi$) from the multiple population viability analysis. More negative values of $\phi$ represent stronger density dependence and a smaller carrying capacity, $K$. Solid lines represent median predicted relationships, and gray shaded areas represent the 95% credible intervals. Vertical hashes on the $x$-axis represent observed values of environmental covariates from the 36 focal streams, red hashes are regulated streams, and black hashes are unregulated streams.

(Kupferberg et al., 2012; Lind et al., 1996). Our findings fit into the larger literature documenting increased health of populations and communities of native species under natural flow regimes (Kiernan et al., 2012; Poff et al., 1997; Tonkin et al., 2018).

Although leveraging existing egg mass survey data is a powerful tool for developing a population dynamics model for a wide-ranging species such as *R. boylii*, we acknowledge that the data we employed were collected for a variety of reasons unrelated to this study's objectives. The focal populations are not a random subset of all *R. boylii* populations. Populations were monitored because they suited a particular researcher's questions, sites were accessible, and frogs were abundant enough

**TABLE 2** Priors and posterior summaries for population growth parameters in the multiple population viability analysis model.

| Parameter | Description | Prior | Mean | SD | 2.5% | 97.5% | SSeff | $\widehat{R}$ |
|---|---|---|---|---|---|---|---|---|
| $\alpha_r$ | Mean intrinsic growth rate | $N(0,5)$ | 0.230 | 0.070 | 0.098 | 0.372 | 5573 | 1.001 |
| $\beta_{\text{tot},t-1}$ | Total annual streamflow effect on $r$ | $N(0,0.1)$ | 0.065 | 0.029 | 0.008 | 0.123 | 2662 | 1.000 |
| $\beta_{\text{tot},t-\text{rec.lag}}$ | Lagged total annual streamflow effect on $r$ | $N(0,0.1)$ | 0.027 | 0.027 | −0.027 | 0.081 | 3692 | 1.002 |
| $\beta_{\text{win},t}$ | Winter peak flow effect on $r$ | $N(0,0.1)$ | −0.025 | 0.030 | −0.084 | 0.033 | 2975 | 1.001 |
| $\beta_{\text{temp}}$ | Mean August stream temperature effect on $r$ | $N(0,0.1)$ | 0.105 | 0.035 | 0.036 | 0.176 | 6133 | 1.001 |
| $\kappa_r$ | SD of region random effect on $r$ | Exp(1) | 0.077 | 0.081 | 0.002 | 0.292 | 7522 | 1.000 |
| $\varepsilon_{r,\text{CC}}$ | Central Coast random effect on $r$ | $N(0,\kappa)$ | 0.019 | 0.077 | −0.119 | 0.204 | 11,060 | 1.000 |
| $\varepsilon_{r,\text{NF}}$ | North Feather random effect on $r$ | $N(0,\kappa)$ | −0.031 | 0.075 | −0.218 | 0.086 | 11,076 | 1.000 |
| $\varepsilon_{r,\text{NC}}$ | North Coast random effect on $r$ | $N(0,\kappa)$ | 0.007 | 0.065 | −0.129 | 0.141 | 7847 | 1.001 |
| $\varepsilon_{r,\text{NSN}}$ | Northern Sierra random effect on $r$ | $N(0,\kappa)$ | −0.009 | 0.072 | −0.170 | 0.131 | 9817 | 1.001 |
| $\varepsilon_{r,\text{SSN}}$ | Southern Sierra random effect on $r$ | $N(0,\kappa)$ | 0.009 | 0.090 | −0.168 | 0.217 | 23,846 | 1.000 |
| $\phi$ | Mean density dependence | $N(0,0.1)$ | −0.009 | 0.002 | −0.013 | −0.005 | 3927 | 1.001 |
| $\theta_{\text{fs}}$ | Effect of forest/shrub cover on $\phi$ | $N(0,0.032)$ | 0.002 | 0.002 | −0.002 | 0.005 | 6313 | 1.000 |
| $\theta_{\text{roc}}$ | Linear effect of spring flow rate of change on $\phi$ | $N(0,0.032)$ | 0.002 | 0.001 | −0.001 | 0.004 | 5101 | 1.001 |
| $\theta_{\text{roc2}}$ | Quadratic effect of spring flow rate of change on $\phi$ | $N(0,0.032)$ | −0.001 | 0.002 | −0.004 | 0.002 | 3053 | 1.001 |
| $\theta_{MP}$ | Effect of streamflow seasonality on $\phi$ | $N(0,0.032)$ | 0.005 | 0.002 | 0.000 | 0.009 | 7526 | 1.000 |
| $\theta_{\text{power}}$ | Effect of streamflow predictability on $\phi$ | $N(0,0.032)$ | 0.003 | 0.003 | −0.003 | 0.010 | 4272 | 1.000 |
| $\omega_{\sigma,\text{unreg}}$ | Mean environmental stochasticity, unregulated streams | Exp(1) | 0.406 | 0.177 | 0.053 | 0.751 | 5988 | 1.002 |
| $\omega_{\sigma,\text{reg}}$ | Mean environmental stochasticity, regulated streams | Exp(1) | 0.577 | 0.197 | 0.158 | 0.970 | 6293 | 1.001 |
| $\varsigma$ | SD of reach random effect on $\sigma R$ | Exp(1) | 0.214 | 0.091 | 0.076 | 0.430 | 3646 | 1.001 |
| $\xi$ | SD of region random effect on $\mu_\sigma$ | Exp(1) | 0.257 | 0.241 | 0.008 | 0.893 | 5195 | 1.000 |
| $\eta_{\text{R,CC}}$ | Central Coast effect on mean environmental stochasticity | $N(0,\xi)$ | 0.021 | 0.179 | −0.363 | 0.399 | 8238 | 1.001 |
| $\eta_{\text{R,NF}}$ | North Feather effect on mean environmental stochasticity | $N(0,\xi)$ | −0.091 | 0.233 | −0.660 | 0.287 | 11,017 | 1.001 |
| $\eta_{\text{R,NC}}$ | North Coast effect on mean environmental stochasticity | $N(0,\xi)$ | 0.068 | 0.177 | −0.269 | 0.457 | 5394 | 1.001 |
| $\eta_{\text{R,NSN}}$ | N Sierra Nevada effect on mean environmental stochasticity | $N(0,\xi)$ | −0.099 | 0.247 | −0.733 | 0.302 | 6424 | 1.001 |
| $\eta_{\text{R,SSN}}$ | S Sierra Nevada effect on mean environmental stochasticity | $N(0,\xi)$ | 0.176 | 0.336 | −0.305 | 0.980 | 6930 | 1.000 |

*Note*: $N$(mean, SD) represents a normal distribution with mean and SD, Exp(rate) represents an exponential distribution with a rate parameter. Mean, SD, 2.5%, and 97.5% columns are the mean, SD, 2.5th percentile, and 97.5th percentile of the posterior distribution. SSeff is the effective sample size, and $\widehat{R}$ is the potential scale reduction factor.

to be studied, or to fulfill specific management objectives and regulatory obligations as part of hydropower relicensing projects, or because dam operations changed. Basic research to observe natural variation (e.g., Hurdygurdy Creek, Angelo Reserve reach of South Fork Eel, Camp Ohlone reach of Alameda Creek, Mad River) occurred at locations where populations are largely protected but not completely immune from direct and indirect anthropogenic influence (e.g., disturbance from recreation, upstream diversion of water for cannabis cultivation, cattle grazing, and climate change associated multiyear drought). Conservation interventions have

been tested in some of the study populations. Fences were installed to protect breeding sites at Big Carson Creek, and canopy thinning was used to mitigate the effects of riparian tree encroachment. At the regulated Cresta Reach of the North Fork Feather River, there has been an intensive recovery effort including salvaging egg masses from stranding, in situ head-starting in cages that protect embryos and tadpoles from non-native crayfish predators, and supplementing the population with zoo-reared frogs. Beyond the regional hydrologic and climatic drivers that influence population dynamics, we are mindful that idiosyncratic local factors are also important. We did not seek to incorporate this fine-grained detail about the mechanisms at work in each focal population, because our goal was to estimate general relationships between population dynamics and environmental conditions, and not to explain all causes of variation in individual populations. These unmodeled, exogenous environmental factors that may be unique to a specific site are reflected in the residual environmental stochasticity parameters. For modeling the habitat suitability and viability of single populations at a fine scale, other tools exist if sufficient data are available. For example, Railsback et al. (2016) created an individual-based model to evaluate recruitment success of *R. boylii* based on channel morphology, flow hydraulics, and thermal conditions, which can be used to evaluate proposed hydrographs on regulated rivers as well as site designs for channel restoration. If capture–mark–recapture data are available in addition to egg mass counts, an integrated population model can be fit and used to project future population trends (Rose et al., 2021). Currently, such detailed demographic data are only available for three populations of *R. boylii*.

With the many idiosyncratic factors that can influence local population dynamics and the natural variability in *R. boylii* abundance, it is challenging to predict future changes in abundance. The difficulty in predicting the abundance of *R. boylii* based on environmental data alone was evidenced by the goodness-of-fit test when half of the time series of egg mass counts was withheld from the input data for a stream and the predicted egg mass counts were compared with observed counts. The fact that future environmental conditions are unknown adds another layer of uncertainty to projecting future *R. boylii* abundance and population viability. One outstanding factor not addressed in our model is the possibility that inter-annual variation in egg mass counts reflects not only changes in abundance but also changes in the proportion of the adult female population that breeds each year. Still, the relationships between environmental covariates and population growth, density dependence, and environmental stochasticity estimated from the focal streams provide insight into conditions that are likely to facilitate population persistence in the future.

Given the very low egg mass density observed in some regulated streams (e.g., the mainstem Trinity River), how have populations been able to persist at such low densities? One possibility is immigration from unregulated tributaries connected to the larger, regulated river. For the mainstem Trinity River in particular, *R. boylii* reproduction occurs in several unregulated tributaries (e.g., Browns Creek, Canyon Creek, Indian Creek) with warmer summer water temperatures (Wheeler et al., 2015). If populations in large, cold, regulated rivers persist as "sinks" (sensu Pulliam, 1988) subsidized by emigrants from viable populations in tributaries, this could give a misleading impression of the egg mass density necessary to support a viable, self-sustaining population. Adult *R. boylii* move seasonally along stream corridors and can disperse distances >1 km during one active season (Bourque, 2008). Therefore, the continued presence of egg masses in regulated reaches of larger rivers is not necessarily evidence that conditions within that reach itself are suitable for healthy *R. boylii* populations. Future studies quantifying the reproductive contribution of tributary populations to the abundance of frogs in larger rivers could help explain the persistence of populations at low densities and improve the MPVA by explicitly modeling the connectivity among nearby populations.

There was a positive relationship between August stream temperature and the intrinsic population growth rate ($r$), but this relationship likely does not extend to warmer temperatures beyond the range in the focal streams (10.9–23.3°C). Most streams (27 of 36) in our dataset came from northern regions of the species' range, and we lack time series data from warmer breeding sites in the Southern Sierra clade. For example, tadpole-rearing sites on the unregulated Clavey River (not studied here) in the Southern Sierra appear to be at the warmest end of the inhabitable range for *R. boylii*; maximum 30-day mean temperatures at three sites there were at or above 24°C (Catenazzi & Kupferberg, 2017). Model-predicted temperatures in the NorWeST dataset do not capture the localized water temperature at breeding and tadpole-rearing sites within streams (Catenazzi & Kupferberg, 2017) because of the spatial and temporal heterogeneity in water temperature that occurs both longitudinally along a stream segment and laterally across the width of a channel. The optimal temperature for tadpole food assimilation, growth, and survival in *R. boylii* likely peaks around 18–22°C (Catenazzi & Kupferberg, 2018) and declines at higher temperatures (Catenazzi & Kupferberg, 2013, 2017). Temperatures above the optimal range for tadpole development have several potential negative effects. Empirically, die-offs of tadpoles have been observed in conjunction with short-term

spikes in temperature (Catenazzi & Kupferberg, 2013). Furthermore, at warmer temperatures periphyton communities at the base of river food webs that support tadpoles and fish can shift to assemblages of inedible algae or toxic cyanobacteria (Furey et al., 2014; Power et al., 2015). Also, warmer temperatures are positively correlated with the prevalence of parasites harmful to *R. boylii* (Kupferberg, Catenazzi, et al., 2009) and many of the non-native predators that are negatively correlated with *R. boylii* presence (e.g., Centrarchid fish, American bullfrogs) thrive in warmer water (Adams & Pearl, 2007; Hayes & Jennings, 1988). Conversely, cold water releases from dams could mitigate the effects of increasing stream temperatures in some regulated streams, as has been suggested for salmonid fish (Null et al., 2013), but may not replicate stable cool temperatures (Willis et al., 2021). Given the variety of complex ecological factors at play, the effect of warmer water temperatures in streams that are already at or near the optimal temperature for *R. boylii* survival and development cannot be inferred based on the MPVA model alone.

The MPVA model was fit to the best available data on population dynamics in *R. boylii*. Most focal streams were from the wetter North Coast region of California, where multiple long-term population studies have taken place and mean annual precipitation can exceed 300 cm/year; few were from xeric southern latitudes where rainfall totals can be as low as 60 cm/year (Iacobellis et al., 2016). Fitting a model primarily to streams from one region has the potential to lead to poor predictions for streams in other regions if the relationships between population dynamics parameters and environmental covariates differ among regions. We included random effects of region (clade) on the mean population growth rate $r$ and the residual environmental stochasticity parameter ($\sigma_R$) to account for the unequal sample size among regions. Regional effects on $r$ and $\sigma_R$ were minimal in our dataset, despite geographic variation in factors such as rainfall and mean catchment area. If more streams with time series of egg mass counts were available from each region, we could have allowed the slope of the relationship between population parameters and environmental variables to vary across regions. Such region-specific information could give better projections of population dynamics within each genetic clade of *R. boylii*.

We found that streams with greater seasonality of flow supported larger populations that exhibited weaker density dependence. Like many stream-dwelling species in Mediterranean climates (Gasith & Resh, 1999), *R. boylii* is adapted to the seasonal cycles of wet winters and dry summers as well as the inter-annual variability in flow in the streams it inhabits. In California, where the seasonal reassembly of algal-based food webs is sensitive to the timing of scouring flows and the transition from high flows to summer base flows (Power et al., 2008), flow metrics for seasonality have proven to be good predictors of biological stream health in terms of periphyton (the food resource for larval *R. boylii*) and aquatic macroinvertebrates (the food resource for adult *R. boylii*) (Peek et al., 2022). Our findings further support the importance of functional flows for native amphibians as well as the novel use of quantitative flow metrics within an MPVA modeling framework.

Despite *R. boylii* being adapted to a naturally variable system, increases in environmental stochasticity beyond the predictable seasonal variability of the winter flood–summer low baseflow hydrograph could lead to a greater risk of population decline. For example, aseasonal summer pulsed flows on the North Fork Feather River were associated with declining egg mass density (Kupferberg et al., 2012). Increased environmental stochasticity is expected to lead to a higher probability of decline, particularly in populations where density dependence limits abundance (Morris & Doak, 2002; but see Doak et al., 2005). Furthermore, increased environmental stochasticity may disrupt the synchrony between environmental cues and adaptive behaviors of the frogs (such as the timing of oviposition relative to rainfall and spring recession flows). Climate change projections indicate that inter-annual variability in precipitation will increase in California, producing more extreme wet and dry years (Diffenbaugh et al., 2015; Swain et al., 2018), more frequent heavy precipitation events (Gershunov et al., 2019; Polade et al., 2017), and increased seasonal variation in streamflow, with higher flows during the wet period and lower flows in summer (Grantham et al., 2018; Halofsky et al., 2019). Increased environmental variability in the future could result in droughts, floods, and wildfires that place more stress on *R. boylii* populations. Many focal populations in this study, particularly those in regulated streams, persisted at low densities and could be susceptible to extirpation if a series of bad years (e.g., due to drought or ill-timed regulated spring or summer pulse flows) causes repeated recruitment failure. Also, because *R. boylii* has been extirpated from large parts of its range (California Department of Fish and Wildlife, 2019; Hayes et al., 2016; Olson & Davis, 2009), if some geographically or genetically isolated populations decline or go extinct, they are unlikely to be rescued by immigration from nearby populations (Peek et al., 2021), which is expected in a healthy amphibian metapopulation (Grant et al., 2007).

## Summary and conclusions

This study documented key environmental covariates of population dynamics in the stream breeding *R. boylii*.

The use of MPVA allowed sharing of information among streams to estimate general relationships, while simultaneously allowing environmental stochasticity to vary among streams. Populations of *R. boylii* inhabiting cold, regulated rivers with altered streamflow regimes had lower density and higher environmental stochasticity compared with populations inhabiting warmer unregulated streams with greater seasonality of streamflow. Population trends and fluctuations differed among streams within each region and within each stream regulation class. Local stream conditions, surrounding terrestrial habitat, disease prevalence, the presence of non-native predators, and many other factors can all interact to determine whether a single population will grow, remain stable, or decline in the future. Although the MPVA model presented here is not intended to predict the future viability of any single population with certainty, the relationships between population growth and streamflow and stream temperature have implications for the future viability of *R. boylii*. Viable populations are most likely to persist in unregulated streams with predictable seasonal streamflow regimes.

## AUTHOR CONTRIBUTIONS

Data used in this study were collected by Sarah J. Kupferberg, Ryan A. Peek, Don Ashton, James B. Bettaso, Steve Bobzien, Ryan M. Bourque, Koen G. H. Breedveld, Alessandro Catenazzi, Joseph E. Drennan, Earl Gonsolin, Marcia Grefsrud, Andrea E. Herman, Matthew R. House, Matt R. Kluber, Amy J. Lind, Karla R. Marlow, Alan Striegle, Michael van Hattem, Clara A. Wheeler, Jeffery T. Wilcox, and Kevin D. Wiseman. Data analysis and writing were led by Jonathan P. Rose. The first draft of the manuscript was written by Jonathan P. Rose and Sarah J. Kupferberg, and Brian J. Halstead and Ryan A. Peek reviewed and commented on earlier versions of the manuscript. All authors reviewed and approved the final manuscript.

## ACKNOWLEDGMENTS

This project was funded by the U.S. Fish and Wildlife Service, with added support from the USGS Ecosystems Mission Area Species Management Research Program. We thank the many organizations that supported this work: California Department of Fish and Wildlife, East Bay Regional Park District, Eel River Recovery Project, Green Diamond Resource Company, Marin Municipal Water District, Marin Open Space District, Pacific Gas and Electric Company, Placer County Water Agency, the San Francisco Public Utilities Commission, and the U.S. Department of Agriculture Forest Service. We thank Ben Sleeter and Jason Kreitler for sharing land cover change projections and Douglas Leasure for sharing the code for the MPVA model. Ted Grantham provided valuable insight into using modeled streamflow for California streams. We thank Jennifer Rowe for reviewing an earlier version of this manuscript, and two anonymous reviewers for providing constructive feedback. This paper is contribution number 880 of the U.S. Geological Survey Amphibian Research and Monitoring Initiative. Any use of trade, product, or firm names is for descriptive purposes only and does not imply endorsement by the U.S. Government.

## CONFLICT OF INTEREST STATEMENT

The authors declare no conflicts of interest.

## DATA AVAILABILITY STATEMENT

Data (Rose et al., 2023) are available from USGS ScienceBase: https://doi.org/10.5066/P98K2WJI. Code (Rose & Halstead, 2023) is available from GitLab: https://doi.org/10.5066/P9QWX2GR.

## ORCID

*Jonathan P. Rose* https://orcid.org/0000-0003-0874-9166
*Sarah J. Kupferberg* https://orcid.org/0000-0002-7273-712X
*Ryan A. Peek* https://orcid.org/0000-0002-9577-6885
*Alessandro Catenazzi* https://orcid.org/0000-0002-3650-4783
*Andrea E. Herman* https://orcid.org/0000-0002-0006-4843
*Clara A. Wheeler* https://orcid.org/0000-0003-3463-248X
*Jeffery T. Wilcox* https://orcid.org/0000-0002-3271-8514
*Brian J. Halstead* https://orcid.org/0000-0002-5535-6528

## REFERENCES

Adams, A. J., A. P. Pessier, and C. J. Briggs. 2017. "Rapid Extirpation of a North American Frog Coincides with an Increase in Fungal Pathogen Prevalence: Historical Analysis and Implications for Reintroduction." *Ecology and Evolution* 7: 10216–32.

Adams, M. J., and C. A. Pearl. 2007. "Problems and Opportunities Managing Invasive Bullfrogs: Is There Any Hope?" In *Biological Invaders in Inland Waters: Profiles, Distribution, and Threats*, edited by F. Gherardi, 679–693. Dordrecht: Springer.

Băncilă, R. I., A. Ozgul, T. Hartel, T. Sos, and B. R. Schmidt. 2016. "Direct Negative Density-Dependence in a Pond-Breeding Frog Population." *Ecography* 39: 449–455.

Bond, N. 2019. "hydrostats: Hydrologic Indices for Daily Time Series Data." R Package Version 0.2.7. https://CRAN.R-project.org/package=hydrostats.

Bourque, R. M. 2008. "Spatial Ecology of an Inland Population of the Foothill Yellow-Legged Frog (*Rana boylii*) in Tehama County, California." MA thesis, Humboldt State University.

Brooks, S. P., and A. Gelman. 1998. "General Methods for Monitoring Convergence of Iterative Simulations." *Journal of Computational and Graphical Statistics* 7: 434–455.

Bunn, S. E., and A. H. Arthington. 2002. "Basic Principles and Ecological Consequences of Altered Flow Regimes for Aquatic Biodiversity." *Environmental Management* 30: 492–507. https://doi.org/10.1007/s00267-002-2737-0.

California Department of Fish and Wildlife. 2019. *A Status Review of the Foothill Yellow-Legged Frog (Rana boylii) in California*. Report to the Fish and Game Commission. Sacramento, CA: California Department of Fish and Wildlife.

California Fish and Game Commission. 2020. *California Fish and Game Commission Notice of Findings for Foothill Yellow-Legged Frog (Rana boylii)*. Sacramento, CA: California Fish and Game Commission.

Catenazzi, A., and S. J. Kupferberg. 2013. "The Importance of Thermal Conditions to Recruitment Success in Stream-Breeding Frog Populations Distributed across a Productivity Gradient." *Biological Conservation* 168: 40–48.

Catenazzi, A., and S. J. Kupferberg. 2017. "Variation in Thermal Niche of a Declining River-Breeding Frog: From Counter-Gradient Responses to Population Distribution Patterns." *Freshwater Biology* 62: 1255–65.

Catenazzi, A., and S. J. Kupferberg. 2018. "Consequences of Dam-Altered Thermal Regimes for a Riverine Herbivore's Digestive Efficiency, Growth and Vulnerability to Predation." *Freshwater Biology* 63: 1037–48.

Colwell, R. K. 1974. "Predictability, Constancy, and Contingency of Periodic Phenomena." *Ecology* 55: 1148–53.

Cooper, A. R., D. M. Infante, W. M. Daniel, K. E. Wehrly, L. Wang, and T. O. Brenden. 2017. "Assessment of Dam Effects on Streams and Fish Assemblages of the Conterminous USA." *Science of the Total Environment* 586: 879–889.

Coulson, T., G. M. Mace, E. Hudson, and H. Possingham. 2001. "The Use and Abuse of Population Viability Analysis." *Trends in Ecology & Evolution* 16: 219–221.

Dare, G. C., R. G. Murray, D. M. M. Courcelles, J. M. Malt, and W. J. Palen. 2020. "Run-of-River Dams as a Barrier to the Movement of a Stream-Dwelling Amphibian." *Ecosphere* 11: e03207.

Davidson, C., H. B. Shaffer, and M. R. Jennings. 2002. "Spatial Tests of the Pesticide Drift, Habitat Destruction, UV-B, and Climate-Change Hypotheses for California Amphibian Declines." *Conservation Biology* 16: 1588–1601.

de Valpine, P., and A. Hastings. 2002. "Fitting Population Models Incorporating Process Noise and Observation Error." *Ecological Monographs* 72: 57–76.

Dennis, B., and M. L. Taper. 1994. "Density Dependence in Time Series Observations of Natural Populations: Estimation and Testing." *Ecological Monographs* 64: 205–224.

Denwood, M. J. 2016. "runjags: An R Package Providing Interface Utilities, Model Templates, Parallel Computing Methods and Additional Distributions for MCMC Models in JAGS." *Journal of Statistical Software* 71: 1–25.

Diffenbaugh, N. S., D. L. Swain, and D. Touma. 2015. "Anthropogenic Warming Has Increased Drought Risk in California." *Proceedings of the National Academy of Sciences of the United States of America* 112: 3931–36.

Doak, D. F., W. F. Morris, C. Pfister, B. E. Kendall, and E. M. Bruna. 2005. "Correctly Estimating How Environmental Stochasticity Influences Fitness and Population Growth." *The American Naturalist* 166: E14–E21.

Eskew, E. A., S. J. Price, and M. E. Dorcas. 2012. "Effects of River-Flow Regulation on Anuran Occupancy and Abundance in Riparian Zones." *Conservation Biology* 26: 504–512.

Freckleton, R. P., A. R. Watkinson, R. E. Green, and W. J. Sutherland. 2006. "Census Error and the Detection of Density Dependence." *Journal of Animal Ecology* 75: 837–851.

Fuller, T. E., K. L. Pope, D. T. Ashton, and H. H. Welsh. 2011. "Linking the Distribution of an Invasive Amphibian (*Rana catesbeiana*) to Habitat Conditions in a Managed River System in Northern California." *Restoration Ecology* 19: 204–213.

Furey, P. C., S. J. Kupferberg, and A. J. Lind. 2014. "The Perils of Unpalatable Periphyton: *Didymosphenia* and Other Mucilaginous Stalked Diatoms as Food for Tadpoles." *Diatom Research* 29: 267–280.

Gasith, A., and V. H. Resh. 1999. "Streams in Mediterranean Climate Regions: Abiotic Influences and Biotic Responses to Predictable Seasonal Events." *Annual Review of Ecology and Systematics* 30: 51–81.

Gershunov, A., T. Shulgina, R. E. S. Clemesha, K. Guirguis, D. W. Pierce, M. D. Dettinger, D. A. Lavers, et al. 2019. "Precipitation Regime Change in Western North America: The Role of Atmospheric Rivers." *Scientific Reports* 9: 9944.

Gonsolin, T. E. 2010. "Ecological Aspects of Foothill Yellow-Legged Frogs (*Rana boylii*) in the Diablo Mountain Range on Upper Coyote Creek, Santa Clara County, CA." MS thesis, San Jose State University.

Grant, E. H. C., W. H. Lowe, and W. F. Fagan. 2007. "Living in the Branches: Population Dynamics and Ecological Processes in Dendritic Networks." *Ecology Letters* 10: 165–175.

Grant, E. H. C., D. A. W. Miller, and E. Muths. 2020. "A Synthesis of Evidence of Drivers of Amphibian Declines." *Herpetologica* 76: 101–7.

Grant, E. H. C., D. A. W. Miller, B. R. Schmidt, M. J. Adams, S. M. Amburgey, T. Chambert, S. S. Cruickshank, et al. 2016. "Quantitative Evidence for the Effects of Multiple Drivers on Continental-Scale Amphibian Declines." *Scientific Reports* 6: 25625.

Grantham, T. E. W., D. M. Carlisle, G. J. McCabe, and J. K. Howard. 2018. "Sensitivity of Streamflow to Climate Change in California." *Climatic Change* 149: 427–441.

Guzy, J. C., E. A. Eskew, B. J. Halstead, and S. J. Price. 2018. "Influence of Damming on Anuran Species Richness in Riparian Areas: A Test of the Serial Discontinuity Concept." *Ecology and Evolution* 8: 2268–79. https://doi.org/10.1002/ece3.3750.

Hahm, W. J., D. N. Dralle, D. M. Rempe, A. B. Bryk, S. E. Thompson, T. E. Dawson, and W. E. Dietrich. 2019. "Low Subsurface Water Storage Capacity Relative to Annual Rainfall Decouples Mediterranean Plant Productivity and Water Use from Rainfall Variability." *Geophysical Research Letters* 46: 6544–53.

Halofsky, J. E., D. L. Peterson, and J. J. Ho. 2019. *Climate Change Vulnerability and Adaptation in South-Central Oregon*. General Technical Report PNW-GTR-97. Portland, OR: U.S. Department of Agriculture, Forest Service, Pacific Northwest Research Station. 473 pp.

Hayes, M. P., and M. R. Jennings. 1988. "Habitat Correlates of Distribution of the California Red-Legged Frog (*Rana aurora draytonii*) and the Foothill Yellow-Legged Frog (*Rana boylii*): Implications for Management." In *Management of Amphibians, Reptiles, and Small Mammals in North America*, edited by

R. C. Szaro, K. E. Severson, and D. R. Patton, 144–158. Fort Collins, CO: USDA Forest Service, Rocky Mountain Forest and Range Experiment Station.

Hayes, M. P., C. A. Wheeler, A. J. Lind, G. A. Green, and D. C. Macfarlane. 2016. *Foothill Yellow-Legged Frog Conservation Assessment in California*. General Technical Report PSW-GTR-248. Albany, CA: U.S. Department of Agriculture, Forest Service, Pacific Southwest Research Station. 193 pp.

Hobbs, N. T., and M. B. Hooten. 2015. *Bayesian Models: A Statistical Primer for Ecologists*. Princeton, NJ: Princeton University Press.

Huang, X., S. Stevenson, and A. D. Hall. 2020. "Future Warming and Intensification of Precipitation Extremes: A "Double Whammy" Leading to Increasing Flood Risk in California." *Geophysical Research Letters* 47: e2020GL088679.

Iacobellis, S. F., D. R. Cayan, J. T. Abatzoglou, and H. Mooney. 2016. "Climate." In *Ecosystems of California*, edited by H. Mooney and E. Zavaleta, 9–25. Oakland, CA: University of California Press.

Isaak, D. J., S. J. Wenger, E. E. Peterson, J. M. Ver Hoef, D. E. Nagel, C. H. Luce, S. W. Hostetler, et al. 2017. "The NorWeST Summer Stream Temperature Model and Scenarios for the Western U.S.: A Crowd-Sourced Database and New Geospatial Tools Foster a User Community and Predict Broad Climate Warming of Rivers and Streams." *Water Resources Research* 53: 9181–9205.

Jennings, M. R., and M. P. Hayes. 1994. *Amphibian and Reptile Species of Special Concern in California*. Rancho Cordova, CA: California Department of Fish and Game, Inland Fisheries Division.

Jones, K. A., L. S. Niknami, S. G. Buto, and D. Decker. 2022. *Federal Standards and Procedures for the National Watershed Boundary Dataset (WBD)*. Techniques and Methods 11-A3, 5th ed. Reston, VA: U.S. Geological Survey. 54 pp. https://doi.org/10.3133/tm11A3.

Kiernan, J., P. Moyle, and P. Crain. 2012. "Restoring Native Fish Assemblages to a Regulated California Stream Using the Natural Flow Regime Concept." *Ecological Applications* 22: 1472–82.

Knape, J., and P. de Valpine. 2012. "Are Patterns of Density Dependence in the Global Population Dynamics Database Driven by Uncertainty about Population Abundance?" *Ecology Letters* 15: 17–23.

Knape, J., N. Jonzén, and M. Sköld. 2011. "On Observation Distributions for State Space Models of Population Survey Data." *Journal of Animal Ecology* 80: 1269–77.

Kupferberg, S. J. 1996. "Hydrologic and Geomorphic Factors Affecting Conservation of a River-Breeding Frog (*Rana boylii*)." *Ecological Applications* 6: 1332–44. https://doi.org/10.2307/2269611.

Kupferberg, S. J., A. Catenazzi, K. Lunde, A. J. Lind, and W. J. Palen. 2009. "Parasitic Copepod (*Lernaea cyprinacea*) Outbreaks in Foothill Yellow-Legged Frogs (*Rana boylii*) Linked to Unusually Warm Summers and Amphibian Malformations in Northern California." *Copeia* 2009: 529–537.

Kupferberg, S. J., A. J. Lind, and W. J. Palen. 2009. "Pulsed Flow Effects on the Foothill Yellow-Legged Frog (*Rana boylii*): Population Modeling." California Energy Commission Publication Number 500-2009-002a.

Kupferberg, S. J., A. J. Lind, V. Thill, and S. M. Yarnell. 2011. "Water Velocity Tolerance in Tadpoles of the Foothill Yellow-Legged Frog (*Rana boylii*): Swimming Performance, Growth, and Survival." *Copeia* 2011: 141–152.

Kupferberg, S. J., W. J. Palen, A. J. Lind, S. Bobzien, A. Catenazzi, J. Drennan, and M. E. Power. 2012. "Effects of Flow Regimes Altered by Dams on Survival, Population Declines, and Range-Wide Losses of California River-Breeding Frogs." *Conservation Biology* 26: 513–524.

Kwon, H.-H., and U. Lall. 2016. "A Copula-Based Nonstationary Frequency Analysis for the 2012–2015 Drought in California." *Water Resources Research* 52: 5662–75. https://doi.org/10.1111/j.1752-1688.1969.tb04897.x.

Leasure, D. R., S. J. Wenger, N. D. Chelgren, H. M. Neville, D. C. Dauwalter, R. Bjork, K. A. Fesenmyer, et al. 2019. "Hierarchical Multi-Population Viability Analysis." *Ecology* 100: e02538.

Light, T. 2003. "Success and Failure in a Lotic Crayfish Invasion: The Roles of Hydrologic Variability and Habitat Alteration." *Freshwater Biology* 48: 1886–97.

Lind, A. J., H. H. Welsh, and R. A. Wilson. 1996. "The Effects of a Dam on Breeding Habitat and Egg Survival of the Foothill Yellow-Legged Frog (*Rana boylii*) in Northwestern California." *Herpetolical Review* 27: 62–67.

Linnell, M. A., and R. J. Davis. 2021. "Historical Disturbances to Rivers Appear to Constrain Contemporary Distribution of a River-Dependent Frog." bioRxiv:2021.01.22.427759.

Lowe, W. H. 2012. "Climate Change Is Linked to Long-Term Decline in a Stream Salamander." *Biological Conservation* 145: 48–53.

Lowe, W. H., L. K. Swartz, B. R. Addis, and G. E. Likens. 2019. "Hydrologic Variability Contributes to Reduced Survival through Metamorphosis in a Stream Salamander." *Proceedings of the National Academy of Sciences of the United States of America* 116: 19563–70.

McCartney-Melstad, E., M. Gidiş, and H. B. Shaffer. 2018. "Population Genomic Data Reveal Extreme Geographic Subdivision and Novel Conservation Actions for the Declining Foothill Yellow-Legged Frog." *Heredity* 121: 112–125.

McGowan, C. P., N. Allan, J. Servoss, S. Hedwall, and B. Wooldridge. 2017. "Incorporating Population Viability Models into Species Status Assessment and Listing Decisions under the U.S. Endangered Species Act." *Global Ecology and Conservation* 12: 119–130.

McKay, L., T. Bondelid, T. Dewald, J. Johnston, R. Moore, and A. Rea. 2012. *NHDPlus Version 2: User Guide*. Washington, DC: National Operational Hydrologic Remote Sensing Center.

Melbourne, B. A., and A. Hastings. 2008. "Extinction Risk Depends Strongly on Factors Contributing to Stochasticity." *Nature* 454: 100–103.

Molano-Flores, B., and T. J. Bell. 2012. "Projected Population Dynamics for a Federally Endangered Plant under Different Climate Change Emission Scenarios." *Biological Conservation* 145: 130–38.

Morris, W. F., and D. F. Doak. 2002. *Quantitative Conservation Biology. Theory and Practice of Population Viability Analysis*. Sunderland, MA: Sinauer Associates Inc.

Moyle, P. B. 1973. "Effects of Introduced Bullfrogs, *Rana catesbeiana*, on the Native Frogs of the San Joaquin Valley, California." *Copeia* 1973: 18–22.

Null, S. E., S. T. Ligare, and J. H. Viers. 2013. "A Method to Consider whether Dams Mitigate Climate Change Effects on Stream Temperatures." *Journal of the American Water Resources Association* 49: 1456–72.

Olson, D. H., and R. J. Davis. 2009. "Conservation Assessment for the Foothill Yellow-Legged Frog (*Rana boylii*) in Oregon, Version 2.0." USDA Forest Service, Region 6, and USDI Bureau of Land Management Inter-Agency Special Status Species Program.

Oregon Department of Fish and Wildlife (ODFW). 2019. "Oregon Department of Fish and Wildlife Sensitive Species List." https://www.dfw.state.or.us/wildlife/diversity/species/docs/Sensitive_Species_List.pdf.

Pacific Gas and Electric Company. 2020. *Results of 2019 Surveys for Foothill Yellow-Legged Frog (Rana boylii) on the Cresta and Poe Reaches of the North Fork Feather River*. San Anselmo, CA: Garcia and Associates. 73 pp.

Pechmann, J. H. K., D. E. Scott, R. D. Semlitsch, J. P. Caldwell, L. J. Vitt, and J. W. Gibbons. 1991. "Declining Amphibian Populations: The Problem of Separating Human Impacts from Natural Fluctuations." *Science* 253: 892–95.

Peek, R., K. Irving, S. M. Yarnell, R. Lusardi, E. D. Stein, and R. Mazor. 2022. "Identifying Functional Flow Linkages between Stream Alteration and Biological Stream Condition Indices across California." *Frontiers in Environmental Science* 9: 790667.

Peek, R. A. 2018. "Population Genetics of a Sentinel Stream-Breeding Frog (*Rana boylii*)." PhD diss., University of California, Davis.

Peek, R. A., S. M. O'Rourke, and M. R. Miller. 2021. "Flow Modification Associated with Reduced Genetic Health of a River-Breeding Frog, *Rana boylii*." *Ecosphere* 12: e03496.

Plummer, M. 2003. "JAGS: A Program for Analysis of Bayesian Graphical Models Using Gibbs Sampling." In *Proceedings of the 3rd International Workshop on Distributed Statistical Computing (DSC 2003)*. Vienna, Austria.

Poff, N. L., J. D. Allan, M. B. Bain, J. R. Karr, K. L. Prestegaard, B. D. Richter, R. E. Sparks, and J. C. Stromberg. 1997. "The Natural Flow Regime." *BioScience* 47: 769–784.

Poff, N. L., J. D. Olden, D. M. Merritt, and D. M. Pepin. 2007. "Homogenization of Regional River Dynamics by Dams and Global Biodiversity Implications." *Proceedings of the National Academy of Sciences of the United States of America* 104: 5732–37.

Polade, S. D., A. Gershunov, D. R. Cayan, M. D. Dettinger, and D. W. Pierce. 2017. "Precipitation in a Warming World: Assessing Projected Hydro-Climate Changes in California and Other Mediterranean Climate Regions." *Scientific Reports* 7: 10783.

Power, M. E., K. Bouma-Gregson, P. Higgins, and S. M. Carlson. 2015. "The Thirsty Eel: Summer and Winter Flow Thresholds that Tilt the Eel River of Northwestern California from Salmon-Supporting to Cyanobacterially Degraded States." *Copeia* 2015: 200–211.

Power, M. E., M. S. Parker, and W. E. Dietrich. 2008. "Seasonal Reassembly of a River Food Web: Floods, Droughts, and Impacts of Fish." *Ecological Monographs* 78: 263–282.

Pulliam, H. R. 1988. "Sources, Sinks, and Population Regulation." *The American Naturalist* 132: 652–661.

R Core Team. 2022. *R: A Language and Environment for Statistical Computing (Version 4.1.3)*. Vienna: R Foundation for Statistical Computing.

Railsback, S. F., B. C. Harvey, S. J. Kupferberg, M. M. Lang, S. McBain, and H. H. Welsh. 2016. "Modeling Potential River Management Conflicts between Frogs and Salmonids." *Canadian Journal of Fisheries and Aquatic Sciences* 73: 773–784.

Ricker, W. E. 1954. "Stock and Recruitment." *Journal of the Fisheries Research Board of Canada* 11: 559–623.

Roesch, A., and H. Schmidbauer. 2018. "WaveletComp: Computational Wavelet Analysis." R Package Version 1.1. https://CRAN.R-project.org/package=WaveletComp.

Rose, J. P., and B. J. Halstead. 2023. "Code for Multiple Population Viability Analysis of Egg Mass Time Series from the Foothill Yellow-Legged Frogs (*Rana boylii*) in California. U.S. Gelogical Survey Software Release." https://doi.org/10.5066/P9QWX2GR.

Rose, J. P., S. J. Kupferberg, R. A. Peek, D. Ashton, J. B. Bettaso, S. Bobzien, R. M. Bourque, et al. 2023. "Egg Mass Time Series for Foothill Yellow-Legged Frogs (*Rana boylii*) in California." U.S. Geological Survey Data Release. https://doi.org/10.5066/P98K2WJI.

Rose, J. P., S. J. Kupferberg, C. A. Wheeler, P. M. Kleeman, and B. J. Halstead. 2021. "Estimating the Survival of Unobservable Life Stages for a Declining Frog with a Complex Life-History." *Ecosphere* 12: e03381.

Schmidt, B. R., R. I. Băncilă, T. Hartel, K. Grossenbacher, and M. Schaub. 2021. "Shifts in Amphibian Population Dynamics in Response to a Change in the Predator Community." *Ecosphere* 12: e03528.

Sleeter, B. M., D. C. Marvin, D. R. Cameron, P. C. Selmants, A. L. R. Westerling, J. Kreitler, C. J. Daniel, J. Liu, and T. S. Wilson. 2019. "Effects of 21st-Century Climate, Land Use, and Disturbances on Ecosystem Carbon Balance in California." *Global Change Biology* 25: 3334–53.

Sleeter, B. M., T. S. Wilson, E. Sharygin, and J. T. Sherba. 2017. "Future Scenarios of Land Change Based on Empirical Data and Demographic Trends." *Earth's Future* 5: 1068–83.

Smith, D. R., N. L. Allan, C. P. McGowan, J. A. Szymanski, S. R. Oetker, and H. M. Bell. 2018. "Development of a Species Status Assessment Process for Decisions under the U.S. Endangered Species Act." *Journal of Fish and Wildlife Management* 9: 302–320.

Snover, M. L., and M. J. Adams. 2016. "Herpetological Monitoring and Assessment on the Trinity River, Trinity County, California – Final Report." U.S. Geological Survey Open-File Report 2016-1089. 93 pp. https://doi.org/10.3133/ofr20161089.

Staples, D. F., M. L. Taper, and B. Dennis. 2004. "Estimating Population Trend and Process Variation for PVA in the Presence of Sampling Error." *Ecology* 85: 923–29.

Stuart, S. N., J. S. Chanson, N. A. Cox, B. E. Young, A. S. L. Rodrigues, D. L. Fischman, and R. W. Waller. 2004. "Status and Trends of Amphibian Declines and Extinctions Worldwide." *Science* 306: 1783–86.

Swain, D. L., B. Langenbrunner, J. D. Neelin, and A. Hall. 2018. "Increasing Precipitation Volatility in Twenty-First-Century California." *Nature Climate Change* 8: 427–433.

Tonkin, J. D., M. T. Bogan, N. Bonada, B. Rios-Touma, and D. A. Lytle. 2017. "Seasonality and Predictability Shape Temporal Species Diversity." *Ecology* 98: 1201–16. https://doi.org/10.1002/ecy.1761.

Tonkin, J. D., D. M. Merritt, J. D. Olden, L. V. Reynolds, and D. A. Lytle. 2018. "Flow Regime Alteration Degrades Ecological

Networks in Riparian Ecosystems." *Nature Ecology & Evolution* 2: 86–93.

Torrence, C., and G. P. Compo. 1998. "A Practical Guide to Wavelet Analysis." *Bulletin of the American Meteorological Society* 79: 61–78. https://doi.org/10.1175/1520-0477(1998)079<0061:APGTWA>2.0.CO;2.

U.S. Fish and Wildlife Service. 2021a. "Endangered and Threatened Wildlife and Plants; Foothill Yellow-Legged Frog; Threatened Status with Section 4(d) Rule for Two Distinct Population Segments and Endangered Status for Two Distinct Population Segments." *Federal Register* 86: 73914–45.

U.S. Fish and Wildlife Service. 2021b. *Species Status Assessment Report for the Foothill Yellow-Legged Frog (Rana boylii), Version 2.0*. Sacramento, CA: U.S. Fish and Wildlife Service.

U.S. Geological Survey. 2019. "National Hydrography Dataset Plus Version 2.1." https://www.epa.gov/waterdata/get-nhdplus-national-hydrography-dataset-plus-data.

van Hattem, M., W. T. Bean, P. Belamaric, H. Gamblin, J. J. Scherbinski, J. Olson, A. Semerdjian, K. Smith, and I. Widick. 2021. "Foothill Yellow-Legged Frog Breeding Biology in a Semi-Regulated River, Humboldt County, CA." California Fish and Wildlife Special CESA Issue, 205–220.

Van Wagner, T. 1996. "Selected Life-History and Ecological Aspects of a Population of Foothill Yellow-Legged Frogs (*Rana boylii*) from Clear Creek, Nevada County, California." MS thesis, California State University.

Welsh, H. H., and L. M. Ollivier. 1998. "Stream Amphibians as Indicators of Ecosystem Stress: A Case Study from California's Redwoods." *Ecological Applications* 8: 1118–32.

Wenger, S. J., D. R. Leasure, D. C. Dauwalter, M. M. Peacock, J. B. Dunham, N. D. Chelgren, and H. M. Neville. 2017. "Viability Analysis for Multiple Populations." *Biological Conservation* 216: 69–77.

Wheeler, C. A., J. B. Bettaso, D. T. Ashton, and H. H. Welsh, Jr. 2015. "Effects of Water Temperature on Breeding Phenology, Growth, and Metamorphosis of Foothill Yellow-Legged Frogs (*Rana boylii*): A Case Study of the Regulated Mainstem and Unregulated Tributaries of California's Trinity River." *River Research and Applications* 31: 1276–86.

Wheeler, C. A., and H. H. Welsh, Jr. 2008. "Mating Strategy and Breeding Patterns of the Foothill Yellow-Legged Frog (*Rana boylii*)." *Herpetological Conservation and Biology* 3: 128–142.

Willis, A. D., R. A. Peek, and A. L. Rypel. 2021. "Classifying California's Stream Thermal Regimes for Cold-Water Conservation." *PLoS One* 16: e0256286. https://doi.org/10.1371/journal.pone.0256286.

Willson, J. D., and M. E. Dorcas. 2003. "Effects of Habitat Disturbance on Stream Salamanders: Implications for Buffer Zones and Watershed Management." *Conservation Biology* 17: 763–771.

Yarnell, S., R. Peek, G. Epke, and A. Lind. 2016. "Management of the Spring Snowmelt Recession in Regulated Systems." *Journal of the American Water Resources Association* 52: 723–736.

Yarnell, S. M., E. D. Stein, J. A. Webb, T. Grantham, R. A. Lusardi, J. Zimmerman, R. A. Peek, B. A. Lane, J. Howard, and S. Sandoval-Solis. 2020. "A Functional Flows Approach to Selecting Ecologically Relevant Flow Metrics for Environmental Flow Applications." *River Research and Applications* 36: 318–324.

Zimmerman, J. K. H., D. M. Carlisle, J. T. May, K. R. Klausmeyer, T. E. Grantham, L. R. Brown, and J. K. Howard. 2022. *California Unimpaired Flows Database v2.1.0*. San Francisco, CA: The Nature Conservancy. https://rivers.codefornature.org/.

Zweifel, R. G. 1955. *Ecology, Distribution, and Systematics of Frogs of the Rana boylei Group*, Vol. 54, 207–292. Berkeley, CA: University of California Publications in Zoology.

## SUPPORTING INFORMATION

Additional supporting information can be found online in the Supporting Information section at the end of this article.

**How to cite this article:** Rose, Jonathan P., Sarah J. Kupferberg, Ryan A. Peek, Don Ashton, James B. Bettaso, Steve Bobzien, Ryan M. Bourque, et al. 2023. "Identifying Drivers of Population Dynamics for a Stream Breeding Amphibian Using Time Series of Egg Mass Counts." *Ecosphere* 14(8): e4645. https://doi.org/10.1002/ecs2.4645